

**Neuroprotective effects of a novel carnosine-hydrazide derivative on hippocampal CA1
damage after transient cerebral ischemia**

Kei Noguchi, MD †¹; Taha F.S. Ali †^{2,3}; Junko Miyoshi, MD¹; Kimihiko Orito, MD¹;
Tetsuya Negoto, MD¹; Tanima Biswas²; Naomi Taira²; Ryoko Koga²; Yoshinari Okamoto²;
Mikako Fujita⁴; Masami Otsuka²; Motohiro Morioka, MD*¹

¹Department of Neurosurgery, Kurume University, School of Medicine, Fukuoka, Japan

²Department of Bioorganic and Medicinal Chemistry, Kumamoto University,

Kumamoto, Japan

³Department of Medicinal Chemistry, Faculty of Pharmacy, Minia University, Minia, Egypt

⁴Research Institute for Drug Discovery, Kumamoto University, Kumamoto, Japan

† These authors contributed equally to this work

*Corresponding author

Address correspondence and reprint requests to:

Motohiro Morioka

Department of Neurosurgery

Kurume University School of Medicine

67, Asahimachi Kurume City, Fukuoka 830-0011, Japan

Telephone: +81-942-31-7570

Fax: +81-942-38-8179

E-mail address: mmorioka@med.kurume-u.ac.jp

Cover title: Neuroprotective effects of L-carnosine hydrazide

Figure count: 6

Word count: 5,161

Search terms: Animal Models of Human Disease, Ischemic Stroke, Oxidant Stress

Abbreviations:

bilateral common carotid artery occlusion = BCCO; heat shock protein 70 = Hsp70; histidyl

hydrazide = HH; L-Carnosine = L-CAR; L-carnosine hydrazide = CNN; reactive carbonyl

species = RCS; 4-hydroxy-trans-2-nonenal = 4-HNE; reactive oxygen species = ROS;

phosphate-buffered saline = PBS; delayed neuronal death = DND; carnosine-NHNH-Ac =

CNNA; Ac-carnosine-NHNH₂ = ACNN; Ac-carnosine-NHNH-Ac = ACNNA; high-power

field = HPF; attenuated total reflection = ATR; nuclear magnetic resonance = NMR

Abstract

Ischemia-reperfusion injuries produce reactive oxygen species that promote the peroxide lipid oxidation process resulting in the production of an endogenic lipid peroxide, 4-hydroxy-trans-2-nonenal (4-HNE), a highly cytotoxic aldehyde that induces cell death. We synthesized a novel 4-HNE scavenger – a carnosine-hydrazide derivative, L-carnosine hydrazide (CNN) – and examined its neuroprotective effect in a model of transient ischemia.

PC-12 cells were pre-incubated with various doses (0-50 mmol/L) of CNN for 30 min, followed by incubation with 4-HNE (250 μ M). An MTT assay was performed 24 h later to examine cell survival. Transient ischemia was induced by bilateral common carotid artery occlusion (BCCO) in the Mongolian gerbil. Animals were assigned to sham-operated (n = 6), placebo-treated (n = 12), CNN pre-treated (20 mg/kg; n = 12), CNN post-treated (100 mg/kg; n = 11), and histidyl hydrazide (a previously known 4-HNE scavenger) post-treated (100 mg/kg; n = 7) groups. Heat shock protein 70 immunoreactivity in the hippocampal CA1 region was evaluated 24 h later, while delayed neuronal death using 4-HNE staining was evaluated 7 days later.

Pre-incubation with 30 mmol/L CNN completely inhibited 4-HNE-induced cell toxicity.

CNN prevented delayed neuronal death by >60% in the pre-treated group (p < 0.001)

and by >40% in the post-treated group ($p < 0.01$). Histidyl hydrazide post-treatment elicited no protective effect. CNN pre-treatment resulted in high heat shock protein 70 and low 4-HNE immunoreactivity in CA1 pyramidal neurons. Higher 4-HNE immunoreactivity was also found in the placebo-treated animals than in the CNN pre-treated animals.

Our novel compound, CNN, elicited highly effective 4-HNE scavenging activity *in vitro*. Furthermore, CNN administration both pre- and post-BCCO remarkably reduced delayed neuronal death in the hippocampal CA1 region via its induction of heat shock protein 70 and scavenging of 4-HNE.

Keywords: carnosine hydrazide, free radical scavenger, global cerebral ischemia, Mongolian gerbils, hippocampus

1. Introduction

The purpose of neuroprotective therapy during the acute stages of cerebral ischemia is to block cytotoxic processes and protect neurons against toxic molecules to prevent cell death. Reactive carbonyl species (RCS) are cytotoxic substances generated from oxidative stress, including membrane lipid-peroxidation reactions, caused by ischemia/reperfusion injuries in the brain [1]. RCS cause damage to proteins, nucleic acids, and lipids, the chemical modification of which results in cytotoxicity and mutagenicity. In addition to its direct toxic effects, the modification of biomolecules by RCS gives rise to a multitude of adducts and cross-linked proteins that have increasingly been implicated in aging and the pathology of a wide range of human diseases [2,3]. RCS can be classified into three groups: (1) α , β -unsaturated aldehydes, such as 4-hydroxy-*trans*-2-nonenal (4-HNE) and acrolein; (2) keto-aldehydes, such as methylglyoxal; and (3) dialdehydes, such as glyoxal and malondialdehyde [4]. Among these RCS, 4-HNE represents one of the most abundant and highly cytotoxic aldehydes generated during lipid peroxidation. For example, it has been reported that 4-HNE greatly contributes to the delayed neuronal death (DND) of pyramidal cells in the CA1 region of the hippocampus after transient cerebral ischemia [5-7]. Although the cell death cascade might start earlier, morphological DND occurs 4-7 days after ischemic

stroke in the hippocampal CA1 region and ultimately induces DNA fragmentation via apoptotic processes [8-12]. Although this phenomenon is clearly different from necrosis (real infarction; core of infarction) caused by severe ischemia, similar processes can be visualized in brain areas surrounding the necrotic tissue. Thus, various types of 4-HNE-scavenging substances have been examined in attempts to prevent DND.

L-Carnosine (L-CAR, Fig. 1), a natural β -alanyl-L-histidine dipeptide that is widely distributed in skeletal muscle and the central nervous system, was first isolated from skeletal muscle extracts by Gulewitsch et al. at the end of the 19th century [13,14]. In biological tissues, L-CAR acts as an antioxidant and scavenger of RCS; as such, L-CAR may protect tissue from oxidative damage [15,16]. It has been proposed that since L-CAR acts as a natural scavenger of cytotoxic aldehydes, it could be a potent and selective scavenger of the toxic lipid peroxidation product, 4-HNE [17,19]. In contrast, several papers have reported that the histidine analogue, L-histidyl hydrazide (histidyl-NHNH₂, HH, Fig. 1), is more efficient than L-CAR in 4-HNE scavenging and in reducing brain damage [20,21]. The formation of cyclic adduct, L-CAR-4-HNE and HH-4-HNE, is presumed (Fig.1). In this study, we integrated the functional groups of L-CAR and HH (i.e., amino and imidazole groups and hydrazide and imidazole groups, respectively) into one molecule to form L-carnosine hydrazide (L-carnosine-NHNH₂,

CNN), expecting the formation of a tighter bicyclic adduct (Fig. 1). We also designed acetyl derivatives ACNN, CNNA, and ACNNA to investigate the role of the amino and the hydrazide groups of CNN (Fig. 1).

Fig. 1: Structures of L-carnosine (L-Car), L-histidine (L-His), histidyl-NHNH₂ (HH), L-carnosine hydrazide (CNN), and the acetylamino derivatives, Ac-carnosine-NHNH₂ (ACNN); acetylhydrazide derivative, carnosine-NHNH-Ac (CNNA); acetylamino-acetylhydrazide derivative, Ac-carnosine-NHNH-Ac (ACNNA); L-carnosine (L-CAR) together with the proposed structure of the 4-HNE adducts.

2. Results and discussion

2.1. Chemistry

Compounds were prepared as shown in Scheme 1 and 2. L-carnosine was esterified, acetylated and treated with hydrazine hydrate to give ACNN (Scheme 1). DCC condensation of Cbz- β -Ala and His-OMe afforded Cbz-carnosine-Ome which was treated with hydrazine hydrate to give Cbz-carnosine-NHNH₂ (Scheme 2). Removal of Cbz group of Cbz-carnosine-NHNH₂ gave CNN that was further acetylated to give diacetylated ACNNA. Acetylation of Cbz-carnosine-NHNH₂ followed by hydrogenolysis gave monoacetylated CNNA. Detail of the synthesis is given in Supplementary Material.

Scheme 1. Synthesis of ACNN.

a) SOCl₂, MeOH, 0 °C 10 min then reflux 1 h, b) Ac₂O, MeOH, KHCO₃, 0 °C 30 min then rt overnight, c) N₂H₄ · H₂O, EtOH, rt overnight.

Scheme 2. Syntheses of CNN, ACNNA, and CNNA.

a) DCC, CH₂Cl₂, 0 °C 2 h then rt overnight, b) N₂H₄ · H₂O, EtOH, rt overnight, c) H₂, 10% Pd/C, MeOH, rt overnight, d) Ac₂O, MeOH, DIPEA, 0 °C 30 min then rt

overnight.

2.2. Measurement of 4-HNE-quenching activity

The proportion of 4-HNE-quenching activity was calculated by comparing the 4-HNE consumption achieved by each compound with that achieved by CNN (defined as 100%; Fig. 2A, B). Fig. 2A presents the 4-HNE capturing activity of each compound tested after 1 h of incubation. CNN, HH, and carnosine-NHNH-Ac (CNNA) were more potent than L-CAR, while Ac-carnosine-NHNH₂ (ACNN) was less active than L-CAR, and Ac-carnosine-NHNH-Ac (ACNNA) elicited the lowest activity. These findings suggest that the introduction of an acetyl group masked the activity of CNN, demonstrating the significance of the amino and hydrazide groups. Moreover, the amino group may be more important than the hydrazide group since ACNN was less active than CNNA, but the masked hydrazide group elicited some activity because CNNA was more active than L-CAR.

Fig. 2B depicts the time course of 4-HNE-quenching activity by CNN, L-CAR, and HH. While CNN and HH demonstrated similar 4-HNE-capturing rates 1 h after incubation (Fig. 2A), CNN was clearly superior since, after 30 min of incubation, the amount of

4-HNE captured by CNN, HH, and L-CAR corresponded to approximately 90%, 70%, and 20%, respectively.

Fig. 2: Depiction of the 4-hydroxy-trans-2-nonenal (4-HNE)-quenching activity of L-carnosine hydrazide (CNN), Ac-carnosine-NHNH₂ (ACNN), carnosine-NHNH-Ac (CNNA), Ac-carnosine-NHNH-Ac (ACNNA), L-carnosine (L-CAR), L-histidine, and histidyl hydrazide (HH). (A) The 4-HNE-capturing activity of all compounds after 1 h incubation. (B) Time course measurement of the 4-HNE-quenching activity of CNN, L-CAR, and HH.

2.3. Cell culture and MTT assay

Fig. 3 illustrates the protective effect of CNN against 4-HNE in PC-12 cells *in vitro*. Pre-incubated (30 min) CNN did not elicit cell toxicity. Furthermore, CNN was able to penetrate cells, and elicit protective effects in a dose-dependent manner. Additionally, 30 mM CNN elicited a complete protective effect against 250 μM 4-HNE.

Fig. 3: Effect of L-carnosine hydrazide on 4-hydroxy-trans-2-nonenal-induced PC-12

cell death

Cells were treated with various concentrations of L-carnosine hydrazide (CNN) for 30 min followed by 1 day of 4-hydroxy-trans-2-nonenal (4-HNE) exposure. Results from the MTT assays are presented (data from 3-6 different experiments) as means \pm standard deviations. # $p < 0.05$ compared to PC-12 cells exposed to 4-HNE without CNN ($n = 4$); ## $p = 0.052$ compared to PC-12 cells exposed to 4-HNE without CNN ($n = 4$).

2.4. Protective effect of CNN against DND

DND was clearly observed in the CA1 subfield of the hippocampus 7 days after ischemia (Fig. 4 and 5). More specifically, the number of viable neurons was 70.3 ± 4.5 per high-power field (HPF) in the sham-operated group versus 1.4 ± 1.3 per HPF in the placebo-treated group, revealing a statistically significant loss of neurons following bilateral common carotid artery occlusion (BCCO) ($p < 0.05$). Significantly more viable neurons were observed in the CNN pre-administration group (44.9 ± 17.7 per HPF) than in the placebo-treated group ($p < 0.05$; Fig. 3C and Fig. 4). A neuroprotective effect was also observed in the CNN post-administration group (24.9 ± 25.1 neurons/HPF, $p < 0.05$), although this effect was weaker than that observed in the pre-administration

group (Fig. 4D and Fig. 5). In contrast, no significant difference was observed between the HH post-administration and placebo-treated groups (7.4 ± 15.4 neurons/HPF; Fig. 4E and Fig. 5). Together, these findings indicated that, while both CNN administration groups exhibited statistically significant neuroprotective activity, CNN pre-administration tended to be more effective than CNN post-administration. Specifically, pre-administration of CNN elicited a >60% protective effect against DND versus the 40% observed in the post-administration group.

Fig. 4: Neuroprotective effect of L-carnosine hydrazide on the pyramidal neuron layer in the middle CA1 region of the hippocampus 7 days after bilateral common carotid artery occlusion

Sections stained with hematoxylin-eosin from (A) sham-operated, (B) placebo-treated, (C) L-carnosine hydrazide (CNN)-treated pre-bilateral common carotid artery occlusion (BCCO), (D) CNN-treated post-BCCO, and (E) histidyl hydrazide (HH)-treated post-BCCO animals. Magnification 400 \times , scale bar 20 μ m.

Fig. 5: Histogram representing the number of viable CA1 pyramidal neurons (neurons/high-power field) in each treatment group. Statistical differences were

determined with a Student's t-test. *** $p < 0.001$ compared to the sham-operated group; ### $p < 0.001$ compared to the placebo-treated group; ## $p < 0.01$ compared to the placebo-treated group. Sham = sham-operated group; placebo = placebo-treated group; CNN pre = L-carnosine hydrazide pre-administration group; CNN post = L-carnosine hydrazide post-administration group; HH post = histidyl hydrazide post-administration group. Each value is expressed as mean \pm SD.

2.5. Evaluation of immunostaining

Representative photographs of 4-HNE and heat shock protein 70 (Hsp70) immunostaining in the hippocampal CA1 region at 24 h after BCCO induction are presented in Fig. 6. Higher 4-HNE immunoreactivity was observed in the cytoplasm of pyramidal neurons in the placebo-treated group than in the CNN pre-administration group. In contrast, the CNN pre-administration group exhibited higher concentrations of Hsp70 immunoreactivity in the cell cytoplasm of pyramidal neurons than did the placebo-treated group.

Fig. 6: Representative photograph of 4-hydroxy-trans-2-nonenal and heat shock protein

70 immunostaining of the pyramidal neuron layer in the middle CA1 region of the hippocampus 24 h after bilateral common carotid artery occlusion

Higher 4-hydroxy-trans-2-nonenal (4-HNE) immunoreactivity was observed in the cytoplasm of pyramidal neurons in tissue from a placebo-treated animal than in that from an animal that received L-carnosine hydrazide (CNN) prior to bilateral common carotid artery occlusion (BCCO) (arrow head). CNN pre-administration resulted in higher heat shock protein 70 (Hsp70) immunoreactivity than did placebo treatment.

Sections were stained with anti-4-HNE antibody and anti-Hsp70 antibody.

Magnification 400×, scale bar 20 μm.

2.6. Discussion

Our study demonstrated that the novel derivative, CNN, had significant neuroprotective effects against DND (by scavenging 4-HNE and preserving Hsp70 induction) in the hippocampal CA1 region of Mongolian gerbils following temporary bilateral occlusion of the common carotid artery.

We synthesized three new derivatives of CNN, namely ACNN, CNNA, and ACNNA (Fig. 1), and confirmed that CNN had the most potent 4-HNE-quenching activity. The

superiority of CNN was due to the the reactivity of the amino and hydrazide groups to form a covalent bond with 4-HNE. We found that CNN was more potent than the previously well-known scavengers, HH, L-histidine, and L-CAR (Fig. 2) [17-23].

The efficacy of HH in protecting neurons against 4-HNE toxicity has been demonstrated in several papers. For example, Guiotto et al. reported that the histidine analogue, HH, is more efficient than carnosine in eliciting aldehyde-sequestering effects and in protecting SH-SY5Y neuroblastoma cells and rat hippocampal neurons from 4-HNE-mediated death [21]. Tang et al. also reported HH as being effective in reducing brain damage and improving functional outcome in a mouse model of focal ischemic stroke [20]. In the current study, we found that the 4-HNE-quenching activities of CNN and HH were similar after 60 min of incubation (Fig. 2A). However, after only 20 min of incubation, the activity of CNN was remarkably higher than that of HH (e.g. 80% of CNN vs 60% of HH, Fig. 2B). The reason for this disparity likely lies in the fact that CNN is able to rapidly and tightly react with 4-HNE to form a bicyclic adduct using its three functional groups (i.e., amino, imidazole, and hydrazide), while HH captures 4-HNE gradually and loosely with only “two hands” (imidazole and hydrazide). This difference in reaction rate is important, because RCS are generated rapidly after ischemic insult. Indeed, although HH exhibited high 4-HNE scavenging activity

(similar to CNN after 60 min incubation) *in vitro*, no difference in scavenging activity was observed when animals were post-treated with HH in our *in vivo* study. Together, these findings suggest that pre-administration of HH may be effective against DND; however, since we aimed to apply our novel CNN derivatives to actual clinical conditions (i.e., after the onset of ischemia), we did not evaluate HH prior to the induction of BCCO. In contrast, CNN elicited a significant neuroprotective effect against DND, even after the onset of ischemia; this result is of great clinical significance.

Alongside our evaluation of 4-HNE-quenching activity, we examined 4-HNE and Hsp70 immunostaining to elucidate how CNN prevented DND. Previously, 4-HNE was proposed to be an important marker of radical-induced lipid peroxidation during cerebral post-ischemic reperfusion injury [17-19,24]. Hsp70 is expressed at low levels in the normal brain but is upregulated under conditions of oxidative stress, such as in the penumbra during the hyperacute stage of stroke [25,26]. Hsp70 is well known for its cytoprotective role against acute ischemic stroke [27,28], and the possibility of a correlation between Hsp70 expression and increased tolerance to ischemia has been reported [29-32]. In the current study, we found that, compared to placebo treatment, CNN administration reduced 4-HNE and increased Hsp70 immunoreactivity. This result

might be explained by the well-established “calpain-cathepsin hypothesis” [33-36], which states that ischemia induces Ca^{2+} mobilization and Ca^{2+} -induced calpain activation. Calpain plays a major role in lysosomal rupture, and lipid peroxidation after ischemic re-perfusion produces 4-HNE that carbonylates Hsp70 at the lysosomal membrane. Carbonylation of Hsp70 leads to not only loss of its chaperone function, but also vulnerability to calpain cleavage. Lysosomal membrane damage is most remarkable when Ca^{2+} -induced calpain activation and 4-HNE-induced Hsp70 carbonylation function in parallel. Consequently, the loss of normal (non-carbonylated) Hsp70 results in the rupture or permeabilization of lysosomal membranes and cathepsin release. These reactions all occur specifically in the CA1 region of the hippocampus and can be the trigger of CA1-related neuronal death.

The limitation of CNN is the relatively high dose 100 to 200 mg/kg in animal experiments. This could be overcome by structure modification of CNN to improve the brain migration property.

3. Conclusion

This study demonstrated that our newly developed carnosine-hydrazide derivative elicited high 4-HNE-scavenging activity, with CNN exhibiting highly effective scavenging activity *in vitro*. CNN administration in Mongolian gerbils also remarkably reduced DND in the CA1 region of the hippocampus after transient cerebral ischemia induced by temporary BCCO. The highly effective scavenging ability of CNN could be due to its ability to prevent 4-HNE-induced Hsp70 carbonylation. As 4-HNE has been implicated in many neurodegenerative disorders, these novel derivatives may be effective in treating a number of diseases associated with 4-HNE pathogenesis, such as Alzheimer's disease, Parkinson's disease, amyotrophic lateral sclerosis, and cardiovascular diseases such as atherosclerosis and stroke [20,37-41]. We are currently developing CNN derivatives to improve the pharmacokinetic property and to extend the utility of CNN.

4. Methods

4.1. General information

All procedures in this study were carried out in strict accordance with the Welfare and Management of Animals Act (Act No. 105 of 1973); standards relating to the Care and Keeping and Reducing Pain of Laboratory Animals (Notice of the Ministry of the Environment No. 84 of 2013); Fundamental Guidelines for Proper Conduct of Animal Experiments and Related Activities in Academic Research Institutions under the jurisdiction of the Ministry of Education, Culture, Sports, Science and Technology (Notice of the Ministry of Education, Culture, Sports, Science and Technology, No. 71 of 2006); Guidelines for Proper Conduct of Animal Experiments (Science Council of Japan, 2006); Methods of Destruction of Animals (Notice of the Ministry of the Environment No. 105 of 2007); and the guidelines for animal experimentation from the Animal Research Center of Kurume University.

All animal experiments were reviewed by the Institutional Animal Care and Use Committee and approved by the president of Kurume University (IACUC #2016-172, #2017-033). All induction was performed under anesthesia, and all efforts were made to minimize suffering.

Statistical analysis was performed using JMP® Pro13 software (SAS Institute Inc., Cary,

NC, USA). A Student's t-test was applied to compare the number of surviving neurons in the CA1 of each of the five groups. Data are presented as mean \pm standard deviation (SD). A p-value of < 0.05 was considered significant.

4.2. Animals

Adult male Mongolian gerbils (MON/JmsGbs, Nihon SLC Co., Shizuoka, Japan), weighting 60-100 g, were used for all experiments. The gerbils were kept in a controlled environment ($22 \pm 2^\circ\text{C}$, $55 \pm 5\%$ humidity) and both laboratory food and tap water were available *ad libitum*. The colony was maintained on a 12 h light/dark cycle, with lights on between 7:00 and 19:00.

4.3. Drugs

In addition to CNN, we designed three acetyl-masked derivatives to study the role of the amino and hydrazide groups, i.e., the acetylamino derivative, ACNN, the acetylhydrazide derivative, CNNA, and the acetylamino-acetylhydrazide derivative, ACNNA (Fig. 1). These compounds were synthesized as described in Scheme 1, 2, and the Supplementary Data Material. The structures of these derivatives were confirmed and their purity was confirmed by high performance liquid chromatography (96-100%).

4.4. Measurement of 4-HNE-quenching activity

In this study, 4-HNE-quenching activity was evaluated by measuring 4-HNE consumption. CNN, ACNN, CNNA, ACNNA, L-CAR, L-histidine, or HH (2 mmol/L) was incubated with 4-HNE (200 μ M) in phosphate-buffered saline (PBS, pH 7.4) at 37°C. The ability of the compounds to capture 4-HNE was evaluated by measuring 4-HNE consumption using high-performance liquid chromatography (CAPCELL PAK C18 UG80 at 37°C, eluted by acetonitrile/10 mM PBS (pH 7.4) (60/40 (v/v)), flow rate 0.50 ml/min). Captured 4-HNE (%) was calculated as follows:

$$\text{Captured 4-HNE (\%)} = 100 - [(A^T/A^0) \times 100]$$

A^0 : 4-HNE peak area at time 0

A^T : 4-HNE peak area at time T

4.5. Cell culture and MTT assay

The rat adrenal pheochromocytoma cell line, PC-12, was maintained in RPNI-1640 (Wako, Osaka, Japan) supplemented with 5% heat-inactivated fetal bovine serum (Biosera, Nuaille, France) and 10% heat-inactivated horse serum (ThermoFisher Scientific, Waltham, MA, USA). PC-12 cells were seeded at 2.5×10^5 cells/well in a

24-well plate in 250 μ L of the culture medium. After 1 day, various concentrations of 2.5 μ L CNN dimethyl sulfoxide solution were added to the medium for 30 min. The culture medium containing CNN was then replaced with fresh, CNN-free medium. Finally, 4-HNE ethanol solution (Merck Millipore, Billerica, MA, USA) was added, and cells were further incubated for another 1 day before the MTT assay was conducted.

4.6. BCCO

Transient cerebral ischemia was induced by temporary BCCO in Mongolian gerbils. Briefly, animals were anesthetized with 2% isoflurane in a mixture of 30% oxygen and 70% nitrous oxide. The common carotid arteries were then dissected from their sheaths via a ventral midline cervical incision and occluded with ligatures for 5 min. After removing the ligatures, the wound was closed. The rectal temperature was maintained between 37.5°C and 38.5°C by a self-regulating heat pad during cerebral ischemia. All procedures were performed accurately under a microscope.

Mongolian gerbils were assigned into five groups: (1) sham-operated group (BCCO was not induced, n = 6), (2) placebo-treated group (2 ml of distilled water was administered intraperitoneally 20 min prior to BCCO, n = 12), (3) CNN pre-administration group (2 mL of CNN [20 mg/kg] was intraperitoneally administered 20 min prior to BCCO, n =

12), (4) CNN post-administration group (2 mL of CNN [100 mg/kg] was intraperitoneally administered immediately after BCCO, n = 11), (5) HH post-administration group (2 mL of HH [100 mg/kg] was intraperitoneally administered immediately after BCCO, n = 7).

4.7. Histopathological evaluation

In order to determine the rate of DND, Mongolian gerbils were perfused with 4% paraformaldehyde in 0.1 M PBS (pH 7.4) following a heparinized saline flash under deep anesthesia with isoflurane 7 days after BCCO. The brains were then removed and post-fixed in the same fixative overnight at 4°C. Brain tissues were embedded in paraffin, and 4 µm-thick, successive coronal sections were prepared using a microtome. Brain sections were stained with hematoxylin-eosin, and hippocampal CA1 damage was evaluated by counting the number of surviving pyramidal neurons within the middle CA1 subfield at high power using a light microscope. Only neurons with visibly normal nuclei were counted.

4.8. Immunohistopathological evaluation

For immunohistopathological evaluation, we compared 4-HNE and Hsp70

immunoreactivity in the hippocampal CA1 region of placebo-treated and CNN pre-administration groups 24 h after the induction of BCCO. Brain sections were prepared in the same manner as those for histopathological evaluation. Then, 4-HNE as an oxidative stress marker was analyzed using antibodies against 4-HNE 1:100 (abcam, Cat. #: ab48506; Cambridge, UK), and Hsp70 as a neuroprotective marker was analyzed using antibodies against Hsp70 1:1000 (abcam, Cat. #: ab181606; Cambridge, UK). All pathological evaluations were performed by two neuropathologists (JM and YS) in independent readings.

Acknowledgements

Source of funding

This work was supported by Grants-in-Aid for Scientific Research from the Ministry of Education, Sports, Science, and Culture of Japan, and by Grants-in-Aid for Challenging Exploratory Research 16K15143 to M. O. from Japan Society of Promotion of Science.

Disclosure

Declarations of interest: none

References

- [1] M. Singh, A. Kapoor, A. Bhatnagar, Oxidative and reductive metabolism of lipid-peroxidation derived carbonyls, *Chem. Biol. Interact.* 234 (2015) 261–273.
- [2] H.M. Semchyshyn, Reactive carbonyl species in vivo: generation and dual biological effects, *Sci. World. J.* (2014) 417842.
- [3] S.W. Hwang, Y.M. Lee, G. Aldini, K.J. Yeum, Targeting Reactive Carbonyl Species with Natural Sequestering Agents, *Molecules.* 21 (2016) 280.
- [4] G. Vistoli, D. De Maddis, A. Cipak, N. Zarkovic, M. Carini, G. Aldini, Advanced glycoxidation and lipoxidation end products (AGEs and ALEs): An overview of their mechanisms of formation, *Free. Radic. Res.* 47 (2013) 3–27.
- [5] T. Urabe, Y. Yamasaki, N. Hattori, M. Yoshikawa, K. Uchida, Y. Mizuno, Accumulation of 4-hydroxynonenal-modified proteins in hippocampal CA1 pyramidal neurons precedes delayed neuronal damage in the gerbil brain, *Neuroscience.* 100 (2000) 241–250.

[6] I. Kruman, A.J. Bruce-Keller, D. Bredesen, G. Waeg, M.P. Mattson, Evidence that 4-hydroxynonenal mediates oxidative stress-induced neuronal apoptosis, *J. Neurosci.* 17 (1997) 5089–5100.

[7] C.H. Lee, K.Y. Yoo, I.K. Hwang, J.H. Choi, O.K. Park, H. Li, et al., Hypothyroid state does not protect but delays neuronal death in the hippocampal CA1 region following transient cerebral ischemia: focus on oxidative stress and gliosis, *J. Neurosci. Res.* 88 (2010) 2661–2668.

[8] T. Kirino, Delayed neuronal death in the gerbil hippocampus following ischemia, *Brain. Res.* 6(239) (1982) 57–69.

[9] W. Zuo, W. Zhang, N. Han, N.H. Chen, Compound IMM-H004, a novel coumarin derivative, protects against CA1 cell loss and spatial learning impairments resulting from transient global ischemia, *C.N.S. Neurosci. Ther.* 21 (2015) 280–288.

[10] A. Heron, H. Pollard, F. Dessi, J. Moreau, F. Lasbennes, Y. Ben-Ari, et al.,

Regional variability in DNA fragmentation after global ischemia evidenced by combined histological and gel electrophoresis observations in the rat brain, *J. Neurochem.* 61 (1993) 1973–1976.

[11] M. Horn, W. Schlote, Delayed neuronal death and delayed neuronal recovery in the human brain following global ischemia, *Acta. Neuropathol.* 85 (1992) 79–87.

[12] T. Iwai, A. Hara, M. Niwa, M. Nozaki, T. Uematsu, N. Sakai, et al., Temporal profile of nuclear DNA fragmentation in situ in gerbil hippocampus following transient forebrain ischemia, *Brain. Res.* 671 (1995) 305–308.

[13] W. Gulewitsch, S. Amiradžibi, Ueber das carnosin, eine neue organische base des fleischextractes, *Ber. Dtsch. Chem. Ges.* 33 (1900) 1902–1903.

[14] M.A. Babizhayev, Biological activities of the natural imidazole-containing peptidomimetics N-acetylcarnosine, carcinine and L-carnosine in ophthalmic and skin care products, *Life. Sci.* 78 (2006) 2343–2357.

- [15] J.H. Cararo, E.L. Streck, P.F. Schuck, G. da C Ferreira, Carnosine and related peptides: therapeutic potential in age-related disorders, *Aging. Dis.* 6(5) (2015) 369.
- [16] G.S. Ribas, C.R. Vargas, M. Wajner, L-carnitine supplementation as a potential antioxidant therapy for inherited neurometabolic disorders, *Gene.* 533(2) (2014) 469–476.
- [17] A. Guiotto, P. Ruzza, M.A. Babizhayev, A. Calderan, Malondialdehyde scavenging and aldose-derived Schiff bases' transglycation properties of synthetic histidyl-hydrazide carnosine analogs, *Bioorg. Med. Chem.* 5 (2007) 6158–6163.
- [18] A.R. Hipkiss, J.E. Preston, D.T. Himswoth, V.C. Worthington, M. Keown, J. Michaelis, et al., Pluripotent protective effects of carnosine, a naturally occurring dipeptide, *Ann. N.Y. Acad. Sci.* 854 (1998) 37–53.
- [19] A.R. Hipkiss, J.E. Preston, D.T. Himswoth, V.C. Worthington, N.J. Abbot, Protective effects of carnosine against malondialdehyde-induced toxicity towards cultured rat brain endothelial cells, *Neurosci. Lett.* 238 (1997) 135–138.

[20] S.C. Tang, T.V. Arumugam, R.G. Cutler, D.G. Jo, T. Magnus, S.L. Chan, et al.,
Neuroprotective actions of a histidine analogue in models of ischemic stroke, *J. Neurochem.* 101 (2007) 729–736.

[21] A. Guiotto, A. Calderan, P. Ruzza, A. Osler, C. Rubini, D.G. Jo, et al., Synthesis
and evaluation of neuroprotective alpha,beta-unsaturated aldehyde scavenger
histidyl-containing analogues of carnosine, *J. Med. Chem.* 48 (2005) 6156–6161.

[22] T. Kawamoto, Y. Ikeda, A. Teramoto, Protective effect of L-histidine (singlet
oxygen scavenger) on transient forebrain ischemia in the rat, *No. To. Shinkei.* 49 (1997)
612–618.

[23] Y. Ikeda, Y. Mochizuki, H. Matsumoto, Y. Nakamura, K. Dohi, H. Jimbo, et al.,
L-histidine but not D-histidine attenuates brain edema following cryogenic injury in rats,
Acta. Neurochir. Suppl. 76 (2000) 195–197.

[24] E. McCracken, D.I. Graham, M. Nilsen, J. Stewart, J.A. Nicoll, K. Horsburgh,

4-Hydroxynonenal immunoreactivity is increased in human hippocampus after global ischemia, *Brain. Pathol.* 11 (2001) 414–421.

[25] J. Ikeda, T. Nakajima, O.C. Osborne, G. Mies, T.S. Nowak Jr., Coexpression of c-fos and hsp70 mRNAs in gerbil brain after ischemia: induction threshold, distribution and time course evaluated by in situ hybridization, *Brain. Res. Mol. Brain. Res.* 26 (1994) 249–258.

[26] H. Kinouchi, F.R. Sharp, J. Koistinaho, K. Hicks, H. Kamii, P.H. Chan, Induction of heat shock hsp70 mRNA and HSP70 kDa protein in neurons in the 'penumbra' following focal cerebral ischemia in the rat, *Brain. Res.* 619 (1993) 334–338.

[27] F.R. Sharp, X. Zhan, D.Z. Liu, Heat shock proteins in the brain: role of Hsp70, Hsp27, and HO-1 (Hsp32) and their therapeutic potential, *Transl. Stroke. Res.* 4 (2013) 685–692.

[28] M.A. Shevtsov, B.P. Nikolaev, L.Y. Yakovleva, A.V. Dobrodumov, A.S. Dayneko, A.A. Shmonin, et al., Neurotherapeutic activity of the recombinant heat shock protein

Hsp70 in a model of focal cerebral ischemia in rats, *Drug. Des. Devel. Ther.* 8 (2014) 639–650.

[29] S. Nishi, W. Taki, Y. Uemura, T. Higashi, H. Kikuchi, H. Kudoh, et al., Ischemic tolerance due to the induction of HSP70 in a rat ischemic recirculation model, *Brain. Res.* 615 (1993) 281–288.

[30] K. Nishino, T.S Nowak Jr., Time course and cellular distribution of hsp27 and hsp72 stress protein expression in a quantitative gerbil model of ischemic injury and tolerance: thresholds for hsp72 induction and hilar lesioning in the context of ischemic preconditioning, *J. Cereb. Blood. Flow. Metab.* 24 (2004) 167–178.

[31] R.W. Currie, J.A. Ellison, R.F. White, G.Z. Feuerstein, X. Wang, F.C. Barone, Benign focal ischemic preconditioning induces neuronal Hsp70 and prolonged astrogliosis with expression of Hsp27, *Brain. Res.* 863 (2000) 169–181.

[32] Y. Liu, H. Kato, N. Nakata, K. Kogure, Temporal profile of heat shock protein 70 synthesis in ischemic tolerance induced by preconditioning ischemia in rat hippocampus,

Neuroscience. 56 (1993) 921–927.

[33] T. Yamashima, Implication of cysteine proteases calpain, cathepsin and caspase in ischemic neuronal death of primates, *Progress. Neurobiol.* 62 (2000) 273–295.

[34] T. Yamashima, S. Oikawa, The role of lysosomal rupture in neuronal death, *Prog. Neurobiol.* 89 (2009) 343–358.

[35] T. Yamashima, Y. Kohda, K. Tsuchiya, T. Ueno, J. Yamashita, T. Yoshioka, et al., Inhibition of ischaemic hippocampal neuronal death in primates with cathepsin B inhibitor CA-074: a novel strategy for neuroprotection based on 'calpain-cathepsin hypothesis', *Eur. J. Neurosci.* 10 (1998) 1723–1733.

[36] T. Yamashima, A.B. Tonchev, C.V. Borlongan, Differential response to ischemia in adjacent hippocampal sectors: neuronal death in CA1 versus neurogenesis in dentate gyrus, *Biotechnol. J.* 2 (2007) 596–607.

[37] E. Mariani, M.C. Polidori, A. Cherubini, P. Mecocci, Oxidative stress in brain

aging, neurodegenerative and vascular diseases: an overview, *J. Chromatogr. B.* 827 (2005) 65–75.

[38] M. Perluigi, R. Coccia, D.A. Butterfield, 4-Hydroxy-2-Nonenal, a Reactive Product of Lipid Peroxidation, and Neurodegenerative Diseases: A Toxic Combination Illuminated by Redox Proteomics Studies, *Antioxid. Redox. Signal.* 17 (2012) 1590–1609.

[39] D.A. Butterfield, M.L. Bader Lange, R. Sultana, Involvements of the lipid peroxidation product, HNE, in the pathogenesis and progression of Alzheimer's disease, *Biochim. Biophys. Acta.* 1801 (2010) 924–929.

[40] V. Ruipérez, F. Darios, B. Davletov, Alpha-synuclein, lipids and Parkinson's disease, *Prog. Lipid. Res.* 49 (2010) 420–428.

[41] E.M. Sajdel-Sulkowska, C.A. Marotta, Alzheimer's disease brain: alterations in RNA levels and in a ribonuclease-inhibitor complex, *Science.* 225 (1984) 947–949.

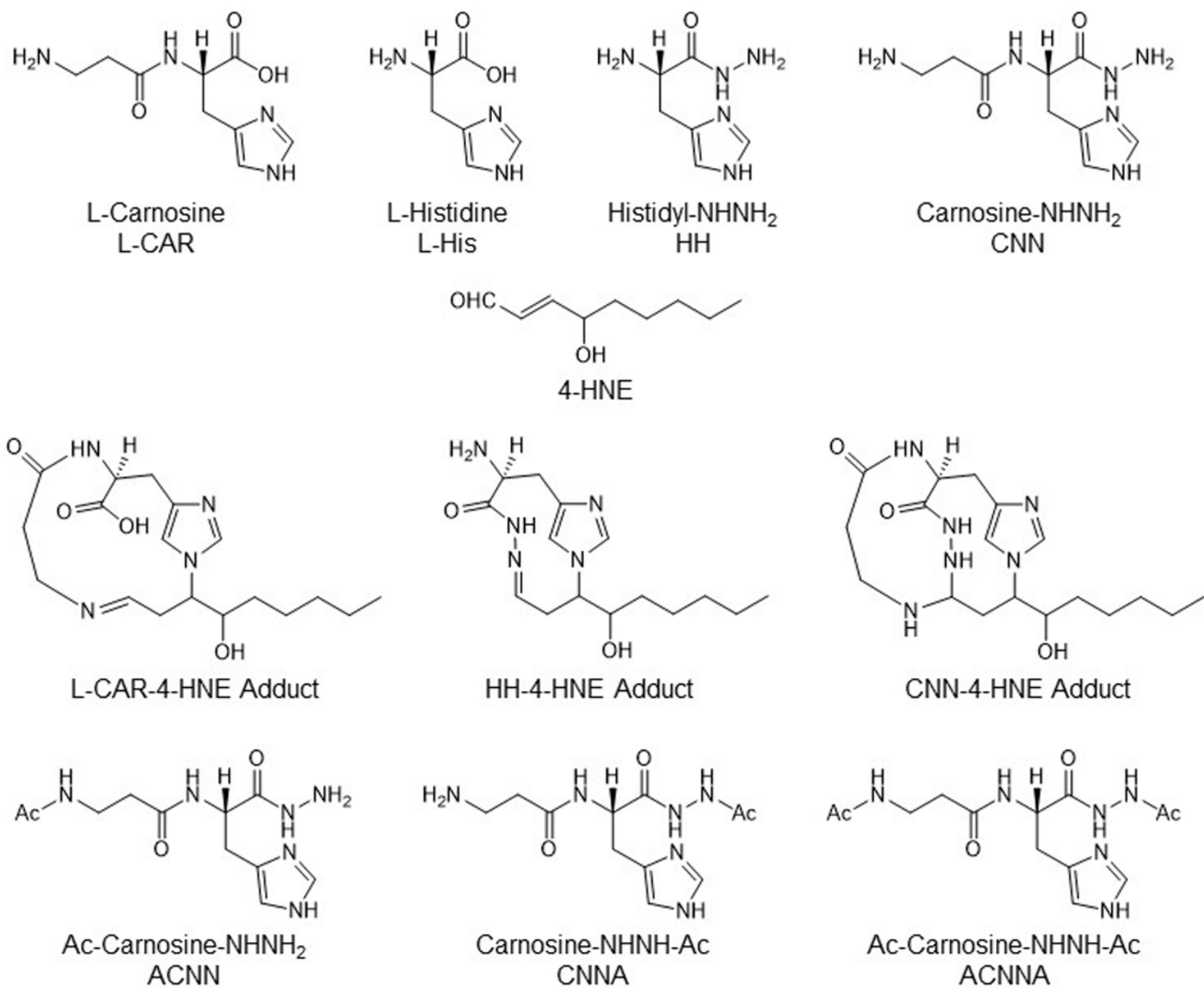


Fig. 1

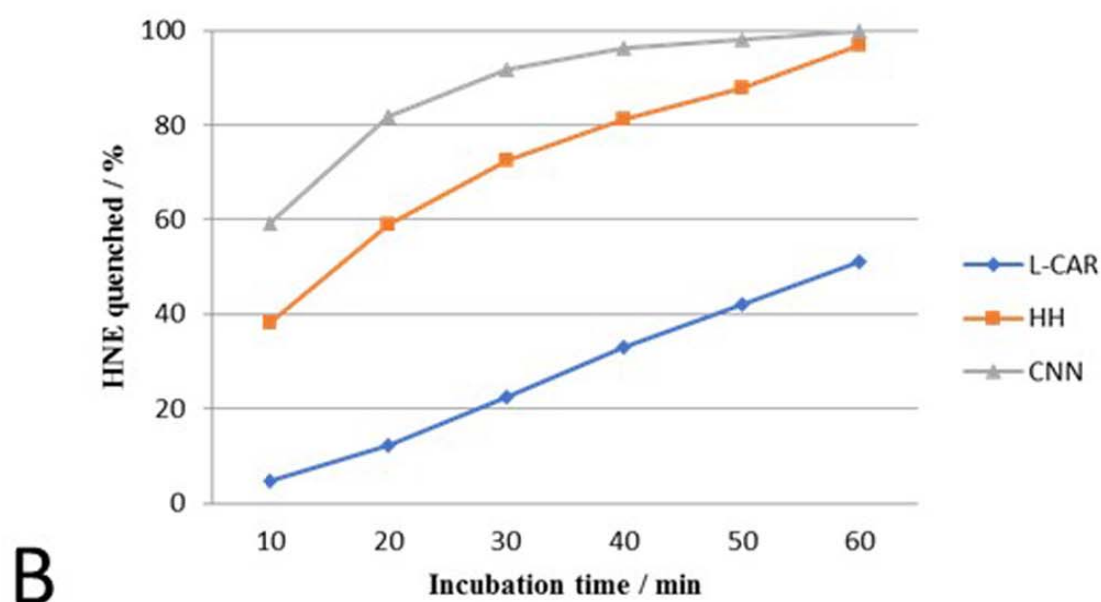
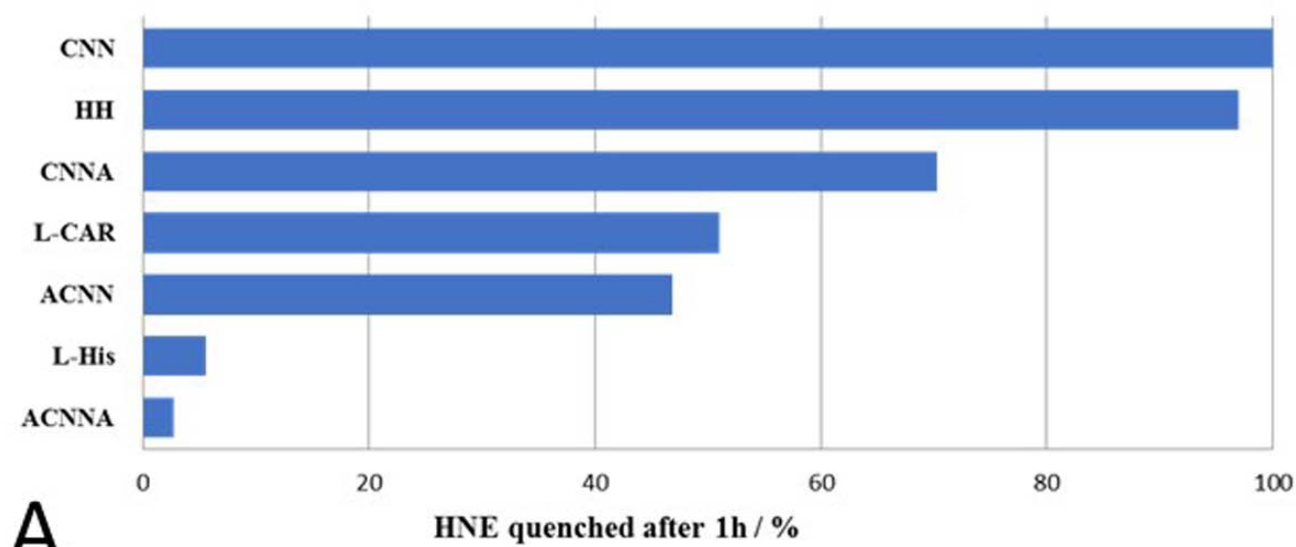


Fig.2

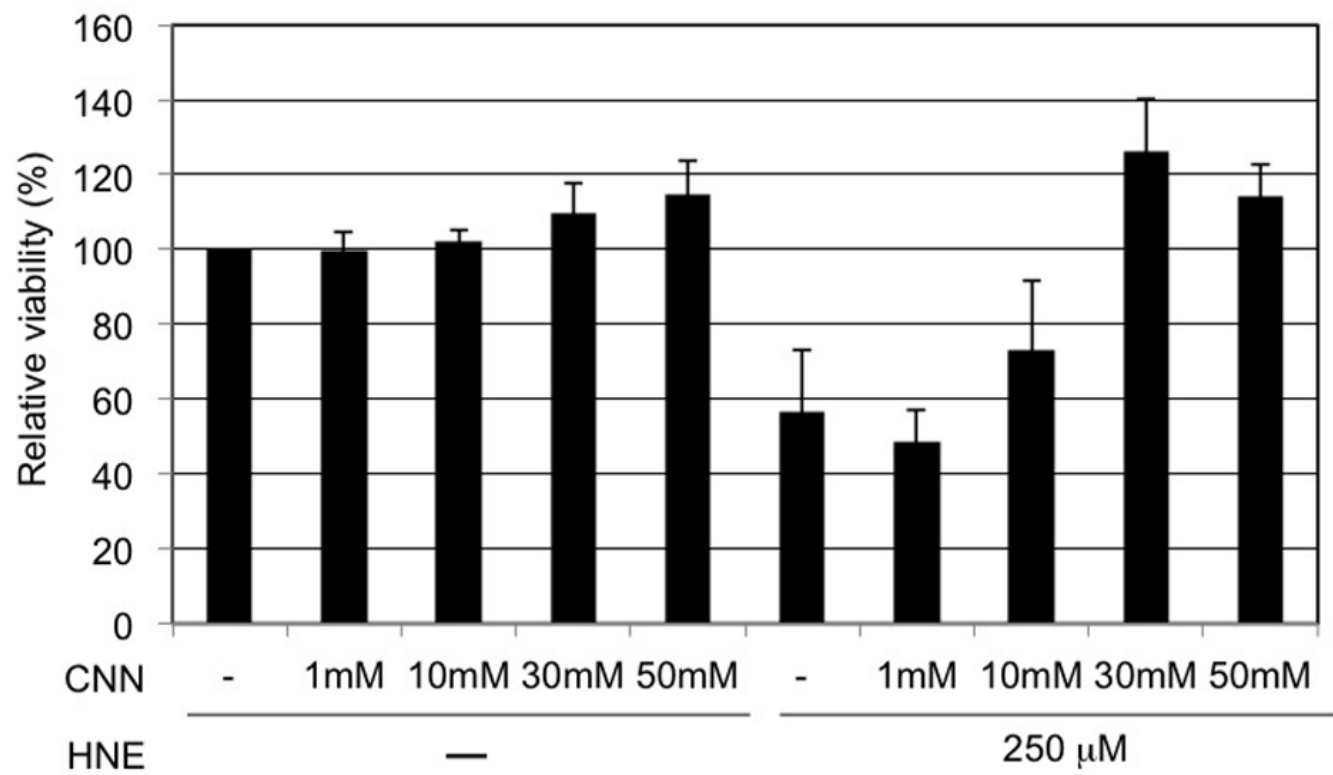


Fig 3

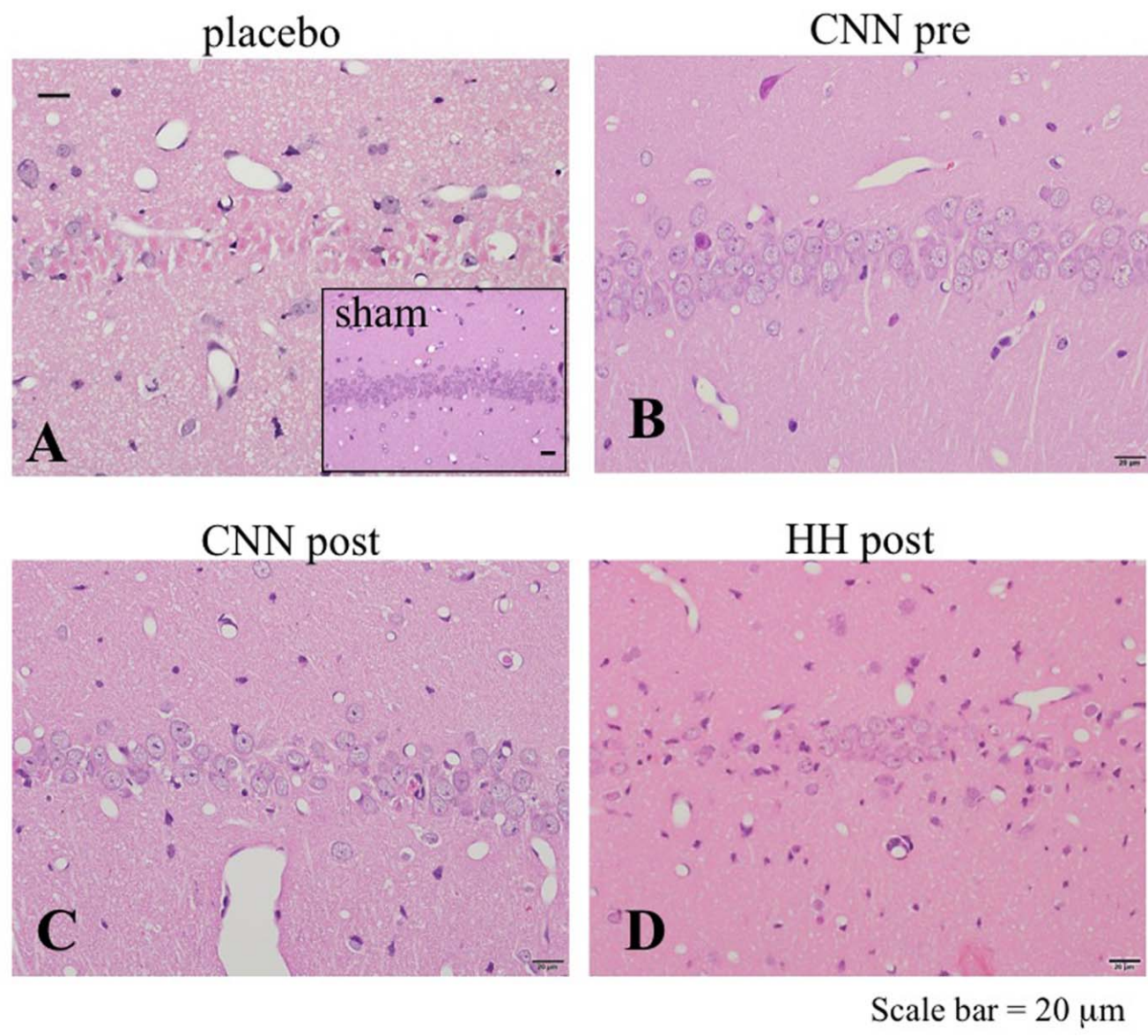


Fig 4

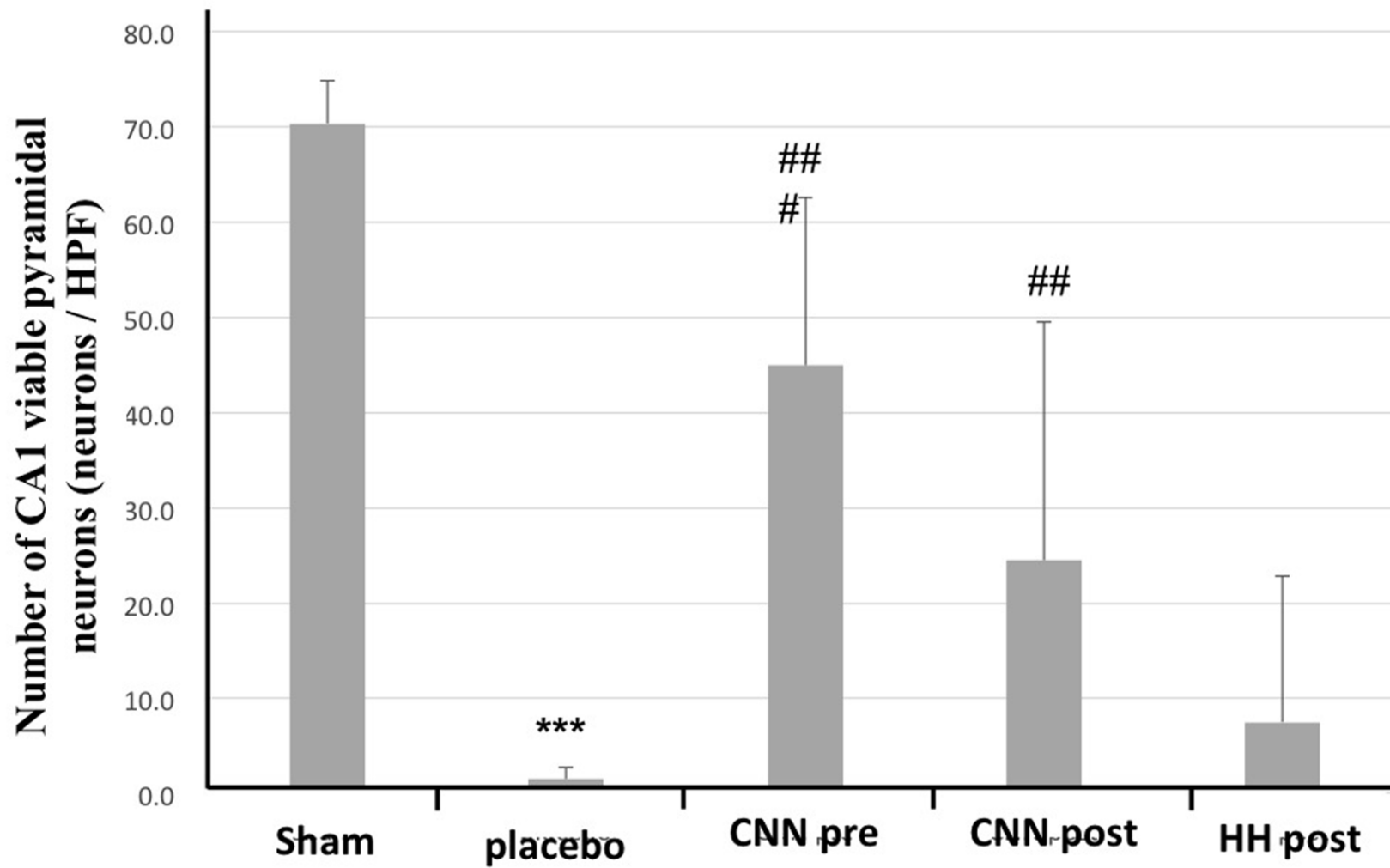


Fig 5

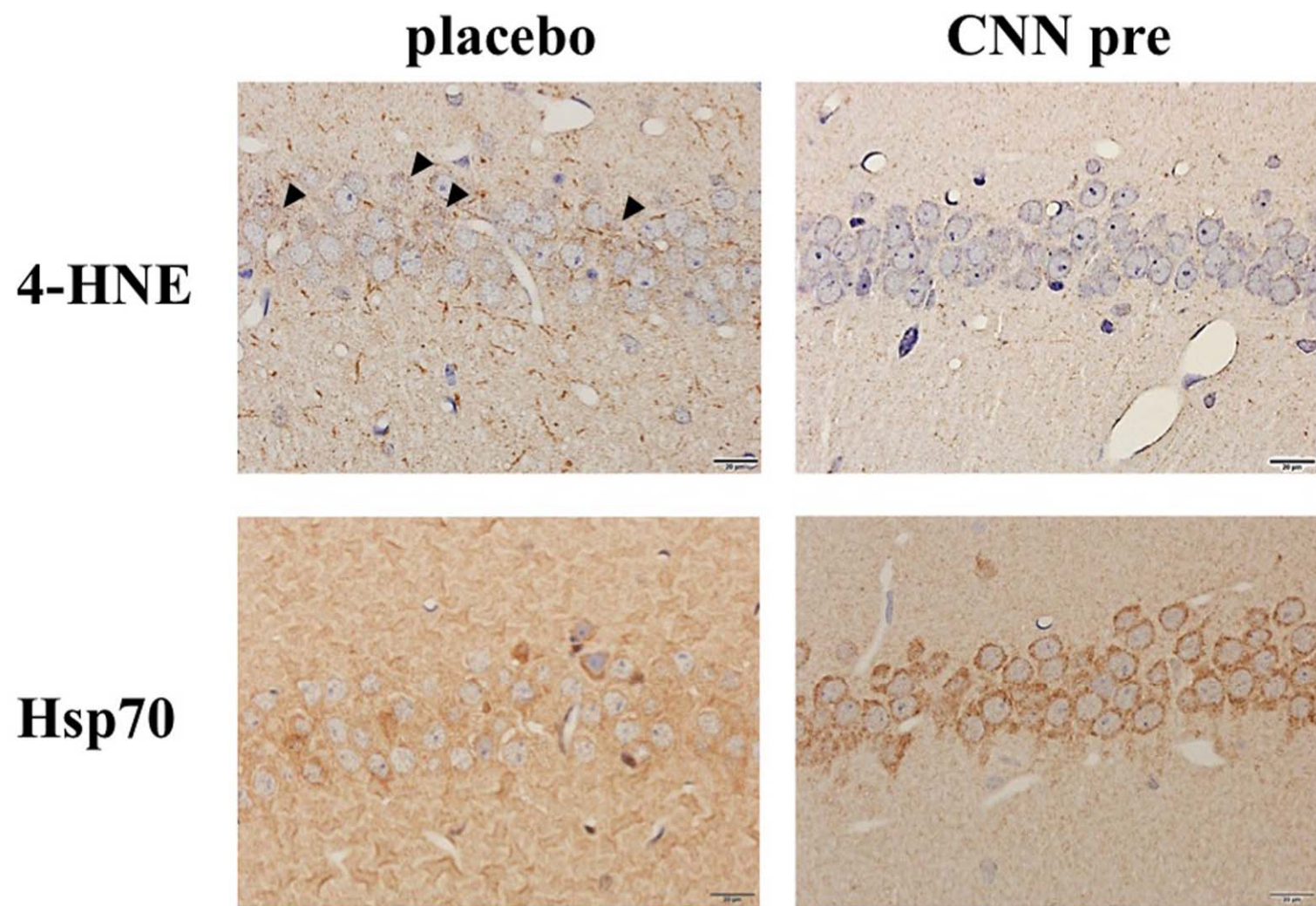


Fig 6

Supplementary Material

Neuroprotective effects of a novel carnosine-hydrazide derivative on hippocampal CA1 damage after transient cerebral ischemia

Kei Noguchi, MD †¹; Taha F.S. Ali †^{2,3}; Junko Miyoshi, MD¹; Kimihiko Orito, MD¹; Tanima Biswas²; Naomi Taira²; Ryoko Koga²; Yoshinari Okamoto²; Mikako Fujita⁴; Masami Otsuka²; Motohiro Morioka, MD*¹

¹Department of Neurosurgery, Kurume University, School of Medicine, Fukuoka, Japan

²Department of Bioorganic and Medicinal Chemistry, Kumamoto University, Kumamoto, Japan

³Department of Medicinal Chemistry, Faculty of Pharmacy, Minia University, Minia, Egypt

⁴Research Institute for Drug Discovery, Kumamoto University, Kumamoto, Japan

† These authors contributed equally to this work

*Corresponding author

Address correspondence and reprint requests to:

Motohiro Morioka

Department of Neurosurgery

Kurume University School of Medicine

67, Asahimachi Kurume City, Fukuoka 830-0011, Japan

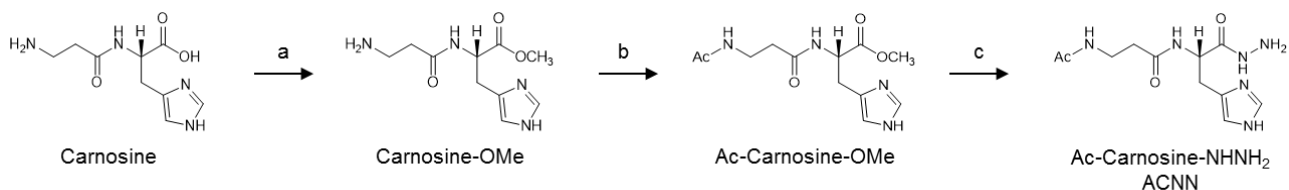
Telephone: +81-942-31-7570

Fax: +81-942-38-8179

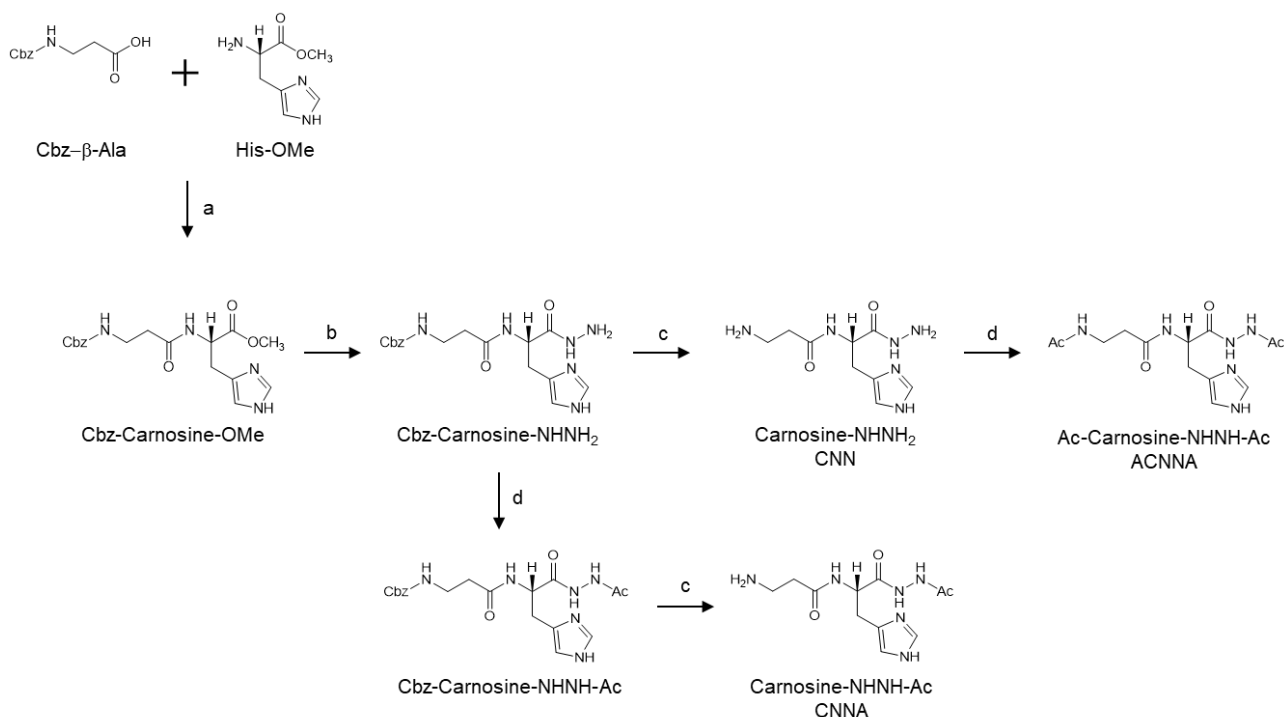
E-mail address: mmorioka@med.kurume-u.ac.jp

Synthesis of L-carnosine hydrazide, Ac-carnosine-NHNH₂, carnosine-NHNH-Ac, and Ac-carnosine-NHNH-Ac

Scheme 1



Scheme 2



General Details

Chemicals were purchased from Aldrich, Fluka, Kanto Chemical, Nacalai Tesque, Tokyo Chemical Industry and Wako. Thin layer chromatography (TLC) was performed on pre-coated plates (Merck TLC sheets silica 60 F₂₅₄ and Fuji silysia chemical Ltd. TLC sheets Chromatorex NH silica). Chromatography was carried out on Silica Gel 60 N (40-100 mesh) (Kanto Chemical) and NH silica gel Chromatorex (NH, 100-200 mesh) (Fuji silysia chemical Ltd.). Nuclear magnetic resonance (NMR) spectra were recorded on a JEOL JNM-AL300 spectrometer. Chemical shifts are referenced to a deuterated solvent signal. Infrared (IR) spectra were recorded on a PerkinElmer Frontier by using the attenuated total reflection (ATR) method. Mass spectra and high-resolution mass spectra (HRMS) were recorded on a JEOL JMS-DX303HF using positive fast atom bombardment (FAB) with 3-nitrobenzyl alcohol as the matrix.

Synthesis of Ac-carnosine-NHNH₂ (ACNN) (Scheme 1)

Carnosine-OMe 2HCl

Thionyl chloride (0.25 ml, 3.3 mM) was added dropwise to a suspension of L-carnosine (447 mg, 2 mM) in MeOH (20 ml) at 0°C. The reaction mixture was stirred at 0°C for 10 min, and then refluxed for 1 h. After cooling to 22 ± 2°C, the solvent was removed *in vacuo*. The product was used in the next step without further purification.

Ac-Carnosine-OMe

Acetic anhydride (1 ml, 10 mM) and KHCO₃ (1 g, 10 mM) were added to a solution of carnosine-OMe 2HCl in MeOH (30 ml) at 0°C under nitrogen atmosphere. The reaction mixture was stirred at 0°C for 30 min, then at 22 ± 2°C overnight. The precipitate was filtered and the solvent was evaporated. The residue was treated with acetone, and the insoluble precipitate was removed by filtration. After evaporation of the solvent, the residue was purified by flash silica gel column chromatography (CH₂Cl₂:MeOH = 4:1) to yield Ac-Carnosine-OMe as a white solid (178 mg, 63%, two steps).

¹H-NMR (300 MHz, CD₃OD) δ 7.68 (s, 1H), 6.92 (s, 1H), 4.70 (dd, *J* = 8.4, 5.4 Hz, 1H), 3.69 (s, 3H), 3.39 (t, *J* = 6.8 Hz, 2H), 3.12 (dd, *J* = 14.8, 5.4 Hz, 1H), 3.01 (dd, *J* = 14.9, 8.4 Hz, 1H), 2.43 (t, *J* = 6.8 Hz, 2H), 1.91 (s, 3H). ¹³C-NMR (75 MHz, CD₃OD) δ 173.8, 173.6, 173.4, 136.5, 134.6, 118.2, 54.0, 52.8, 36.9, 36.3, 29.9, 22.6. IR (ATR) 3305, 2953, 1758, 1630, 1538, 1427, 1212 cm⁻¹. MS (FAB) *m/z* 283.3 (M+H)⁺. HRMS (FAB) : Calcd for C₁₂H₁₉N₄O₄: 283.1406, Found 283.1406

Ac-carnosine-NHNH₂ (ACNN)

Hydrazine monohydrate (1.1 ml, 22 mM) was added to a solution of Ac-Carnosine-OMe (175 mg, 1.1 mM) in EtOH (10 ml), and the reaction mixture was stirred at 22 ± 2°C overnight. The resulting precipitate was filtered, and then washed with EtOH (50 ml) and Et₂O (200 ml) to yield Ac-carnosine-NHNH₂ (ACNN) as a white solid (50 mg, 28%).

¹H-NMR (300 MHz, D₂O) δ 7.66 (s, 1H), 6.93 (s, 1H), 4.49 (dd, *J* = 8.0, 6.8 Hz, 1H), 3.33 (t, *J* = 6.5 Hz, 2H), 3.02 (dd, *J* = 14.8, 6.5 Hz, 1H), 2.93 (dd, *J* = 14.8, 8.4 Hz, 1H), 2.42 (t, *J* = 6.5 Hz, 2H), 1.89 (s, 3H). ¹³C-NMR (75 MHz, D₂O) δ 174.7, 174.6, 172.5, 136.7, 133.5, 117.5, 53.2, 36.1, 35.3, 29.3, 22.2. IR (ATR) 3286, 2922, 1651, 1633, 1623, 1455, 1425 cm⁻¹. MS (FAB) *m/z* 283.3 (M+H)⁺. HRMS (FAB) : Calcd for C₁₁H₁₉N₆O₃ : 283.1519, Found 283.1526.

Synthesis of L-carnosine hydrazide (CNN) (Scheme 2)

Cbz-carnosine-OMe

Dicyclohexylcarbodiimide (500 mg, 2.4 mM) was gradually added to a solution of *N*-carbobenzyloxy-β-alanine (450 mg, 2 mM) and L-histidine methyl ester in CH₂Cl₂ (50 ml) at 0°C. The reaction mixture was stirred at 0°C for 2 h, then at 22 ± 2°C overnight. The resulting precipitate was filtered and the filtrate was washed with aqueous saturated NaHCO₃ (2 x 20 ml). The aqueous layer was

extracted with CH₂Cl₂ (2 x 30 ml), and the combined organic layer was dried over Na₂SO₄. After removal of the solvent *in vacuo*, the residue was purified by silica gel column chromatography (AcOEt:MeOH = 5:1) to yield cbz-carnosine-OMe as a white solid (411 mg, 55%).

¹H-NMR (300 MHz, CD₃OD) δ 7.56 (d, *J* = 1.1 Hz, 1H), 7.33 - 7.26 (m, 5H), 6.86 (s, 1H), 5.05 (s, 2H), 4.68 (dd, *J* = 8.2, 5.5 Hz, 1H), 3.66 (s, 3H), 3.35 (t, *J* = 6.8 Hz, 2H), 3.09 (dd, *J* = 14.9, 5.5 Hz, 1H), 2.98 (dd, *J* = 14.8, 8.2 Hz, 1H), 2.42 (t, *J* = 6.8 Hz, 2H). ¹³C-NMR (75 MHz, CD₃OD) δ 173.9, 173.6, 158.8, 138.4, 136.5, 134.8, 129.6, 129.1, 128.9, 118.1, 67.4, 54.1, 52.8, 38.3, 36.8, 30.0. IR (ATR) 3287, 2952, 1700, 1649, 1251 cm⁻¹. MS (FAB) *m/z* 375.3 (M+H)⁺. HRMS (FAB) : Calcd for C₁₈H₂₃N₄O₅ : 375.1668, Found 375.1670.

Cbz-carnosine-NHNH₂

Hydrazine monohydrate (0.55 ml, 11 mM) was added to a solution of cbz-carnosine-OMe (400 mg, 1.1 mM) in EtOH (30 ml), and the reaction mixture was stirred at 22 ± 2°C overnight. After cooling the mixture to 0°C, the resulting precipitate was filtered, and then washed with EtOH (50 ml) and Et₂O (200 ml) to yield cbz-carnosine-NHNH₂ as a white solid (275 mg, 69%). The product was used in the next step without further purification.

¹H-NMR (300 MHz, CD₃OD) δ 7.56 (d, *J* = 1.1 Hz, 1H), 7.35 - 7.29 (m, 5H), 6.86 (s, 1H), 5.07 (s, 2H), 4.55 (dd, *J* = 8.1, 6.1 Hz, 1H), 3.35 (d, *J* = 6.9 Hz, 2H), 3.04 (dd, *J* = 14.5, 5.9 Hz, 1H), 2.90 (dd, *J* = 14.8, 8.2 Hz, 1H), 2.40 (t, *J* = 6.8 Hz, 2H). ¹³C-NMR (75 MHz, dimethyl sulfoxide) δ 170.7, 170.5, 156.3, 137.4, 134.9, 133.9, 128.6, 128.0, 117.4, 65.4, 51.7, 37.1, 35.7, 29.9. IR (ATR) 3288, 3208, 3032, 2940, 1703, 1660, 1635, 1262 cm⁻¹. MS (FAB) *m/z* 375.3 (M+H)⁺. HRMS (FAB) : Calcd for C₁₇H₂₃N₆O₄ : 375.1781, Found 375.1779.

L-carnosine hydrazide (CNN)

10% Pd/C (75 mg, 20 wt%) was added to a solution of cbz-carnosine-NHNH₂ (375 mg, 1 mM) in MeOH (50 ml). The reaction flask was flashed five times with hydrogen, and then the reaction mixture was stirred at 22 ± 2°C overnight under hydrogen atmosphere. The mixture was filtered through a celite pad, and the residue was washed with MeOH (20 ml). After combining the organic layer, the solvent was removed under reduced pressure. The residue was purified by NH-silica gel column chromatography (AcOEt:MeOH = 2:1) to yield L-carnosine hydrazide (CNN) as a white solid (175 mg, 73%).

¹H-NMR (300 MHz, CD₃OD) δ 7.59 (d, *J* = 1.2 Hz, 1H), 6.87 (d, *J* = 0.9 Hz, 1H), 4.60 (dd, *J* = 8.6, 5.7 Hz, 1H), 3.08 (ddd, *J* = 14.7, 5.7, 0.5 Hz, 1H), 2.98 - 2.81 (m, 3H), 2.34 (td, *J* = 6.5, 2.2 Hz, 2H). ¹³C-NMR (75 MHz, CD₃OD) δ 174.7, 172.9, 136.5, 134.8, 118.4, 53.6, 39.4, 39.1, 30.5. IR (ATR) 3350, 3275, 3179, 3023, 2919, 1631, 1561, 1455, 1425 cm⁻¹. MS (FAB) *m/z* 241.2 (M+H)⁺. HRMS (FAB) : Calcd for C₉H₁₇N₆O₂ : 241.1413, Found 241.1412.

Synthesis of Ac-carnosine-NHNH-Ac (ACNNA) (Scheme 2)

Ac-carnosine-NHNH-Ac (ACNNA)

Acetic anhydride (1.5 ml, 15 mM) and diisopropylethylamine (2 ml, 10.5 mM) were added to a solution of carnosine hydrazide (170 mg, 0.7 mM) in MeOH (30 ml) at 0°C under nitrogen atmosphere. The reaction mixture was stirred at 0°C for 30 min, then at 22 ± 2°C overnight. The resulting precipitate was filtered and the solvent was evaporated *in vacuo*. The residue was purified by silica gel column chromatography (CH₂Cl₂:MeOH = 1:1) to yield Ac-carnosine-NHNH-Ac (ACNNA) as a white solid (125 mg, 55%).

¹H-NMR (300 MHz, CD₃OD) δ 7.59 (d, *J* = 1.1 Hz, 1H), 6.91 (s, 1H), 4.69 (dd, *J* = 8.1, 5.5 Hz, 1H), 3.41 - 3.34 (m, 2H), 3.16 (dd, *J* = 15.1, 5.1 Hz, 1H), 2.97 (dd, *J* = 15.1, 8.0 Hz, 1H), 2.39 (td, *J* = 6.7, 1.5 Hz, 2H), 2.00 (s, 3H), 1.90 (s, 3H). ¹³C-NMR (75 MHz, D₂O) δ 175.3, 175.2, 174.1, 173.5, 137.3, 133.8, 118.5, 53.5, 36.8, 36.0, 30.0, 22.9, 20.9. IR (ATR) 3274, 3178, 3027, 2934, 1634, 1603, 1557, 1486, 1229 cm⁻¹. MS (FAB) *m/z* 325.3 (M+H)⁺. HRMS (FAB) : Calcd for C₁₃H₂₁N₆O₄ : 325.1624, Found 325.1624.

Synthesis of carnosine-NHNH-Ac (CNNA) (Scheme 2)

Cbz-Carnosine-NHNH-Ac

Acetic anhydride (0.5 ml, 5 mM) and diisopropylethylamine (1.5 ml, 8 mM) were added to a solution of Cbz-Carnosine-NHNH₂ (375 mg, 1 mM) in MeOH (20 ml) at 0°C. The reaction mixture was stirred at 0°C for 30 min, then at 22 ± 2°C overnight. The resulting precipitate was filtered and the solvent was evaporated *in vacuo*. The residue was purified by NH-silica gel column chromatography (AcOEt:MeOH = 2:1) to yield cbz-Carnosine-NHNH-Ac as a white solid (330 mg, 79%).

¹H-NMR (300 MHz, CD₃OD) δ 7.56 (d, *J* = 1.0 Hz, 1H), 7.35 - 7.28 (m, 5H), 6.89 (s, 1H), 5.06 (s, 2H), 4.69 (dd, *J* = 8.0, 5.5 Hz, 1H), 3.35 (t, *J* = 5.0 Hz, 2H), 3.15 (dd, *J* = 15.0, 5.3 Hz, 1H), 2.97 (dd, *J* = 14.9, 8.0 Hz, 1H), 2.40 (t, *J* = 6.7 Hz, 2H), 1.99 (s, 3H). ¹³C-NMR (75 MHz, CD₃OD) δ 173.9, 172.7, 172.3, 158.9, 138.4, 136.5, 133.7, 129.6, 129.1, 128.9, 119.4, 67.5, 53.2, 38.3, 37.0, 30.3, 20.4. IR (ATR) 3189, 3033, 2901, 1686, 1638, 1602, 1484, 1264, 1230 cm⁻¹. MS (FAB) *m/z* 417.3 (M+H)⁺. HRMS (FAB) : Calcd for C₁₉H₂₅N₆O₅ : 417.1886, Found 417.1892.

Carnosine-NHNH-Ac (CNNA)

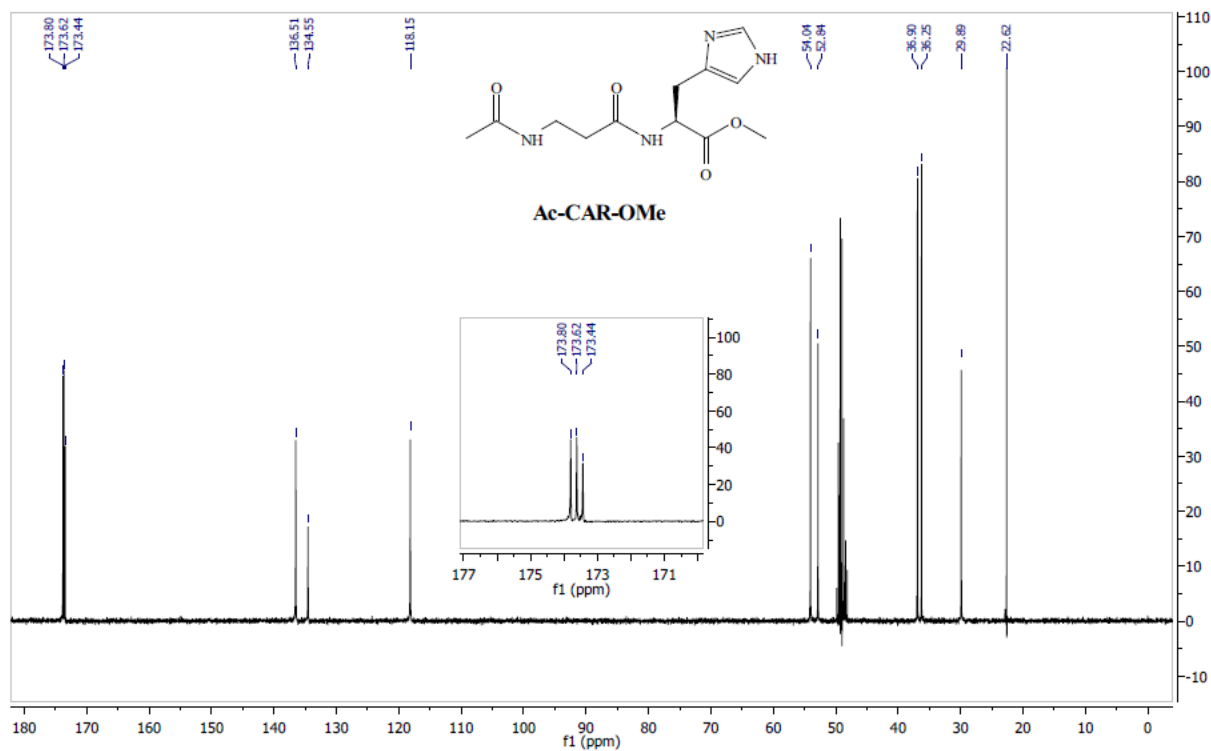
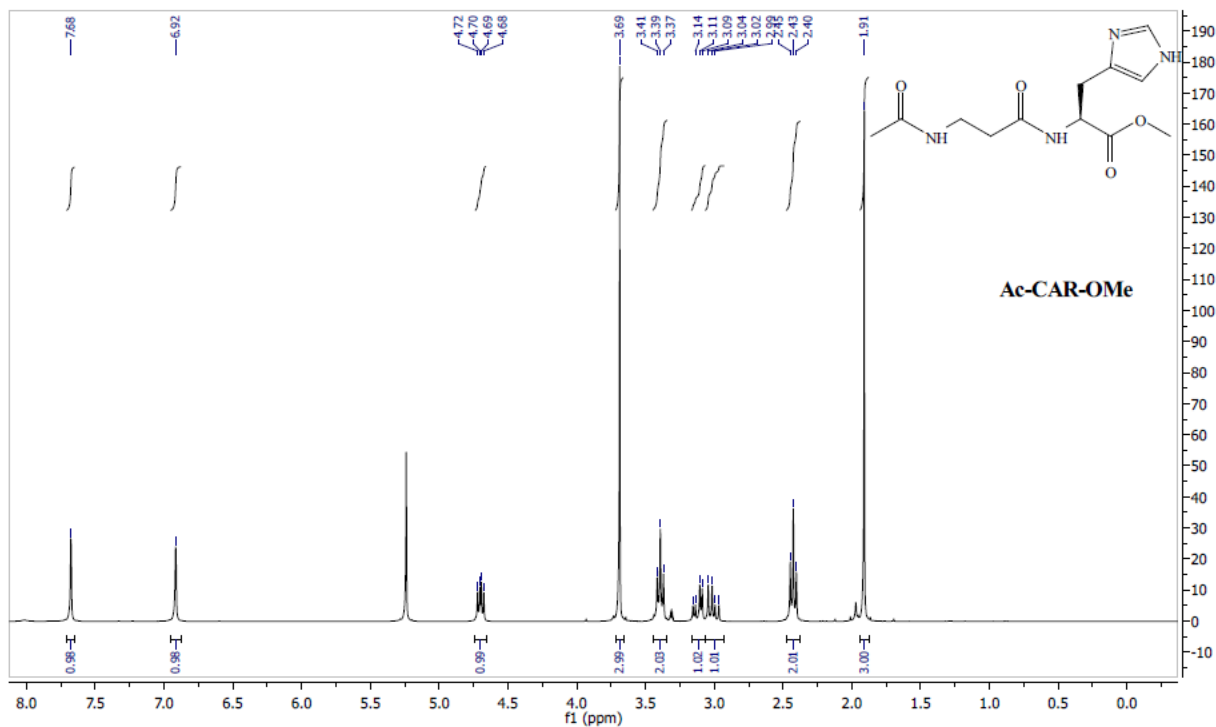
10% Pd/C (66 mg, 20 wt%) was added to a solution of cbz-Carnosine-NHNH-Ac (330 mg, 0.8 mM) in MeOH (25 ml). The reaction flask was flashed five times with hydrogen, then the reaction mixture was stirred at 22 ± 2°C overnight under hydrogen atmosphere. The mixture was filtered through a celite pad, and the residue was washed with MeOH (20 ml). After combining the organic layer, the solvent was removed under reduced pressure. The residue was purified by NH-silica gel column chromatography (AcOEt:MeOH = 2:1) to yield Carnosine-NHNH-Ac (CNNA) as a white solid (180 mg, 80%).

¹H-NMR (300 MHz, CD₃OD) δ 7.58 (d, *J* = 1.1 Hz, 1H), 6.90 (d, *J* = 0.9 Hz, 1H), 4.71 (dd, *J* = 8.3, 5.2 Hz, 1H), 3.18 (dd, *J* = 14.7, 5.5 Hz, 1H), 2.98 (dd, *J* = 15.0, 8.3 Hz, 1H), 2.87 (t, *J* = 6.4 Hz, 2H), 2.36 (td, *J* = 6.4, 3.1 Hz, 2H), 1.99 (s, 3H). ¹³C-NMR (75 MHz, CD₃OD) δ 174.6, 172.5, 172.0, 136.5,

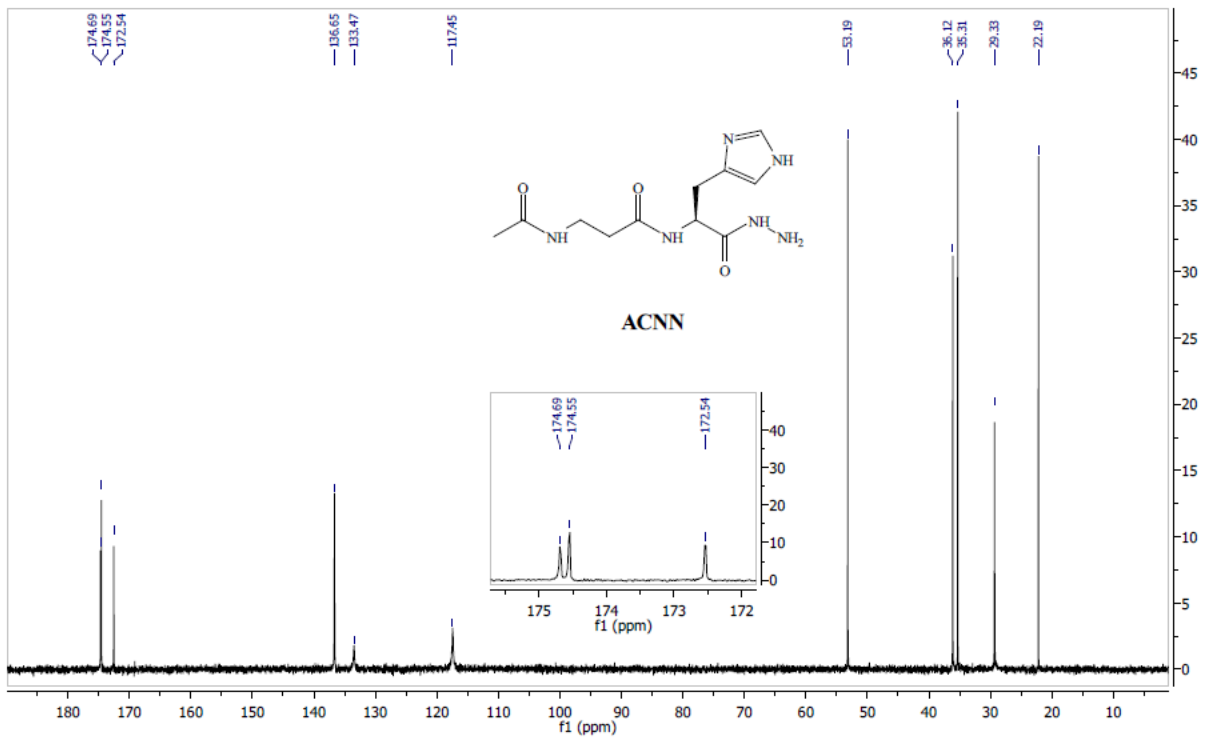
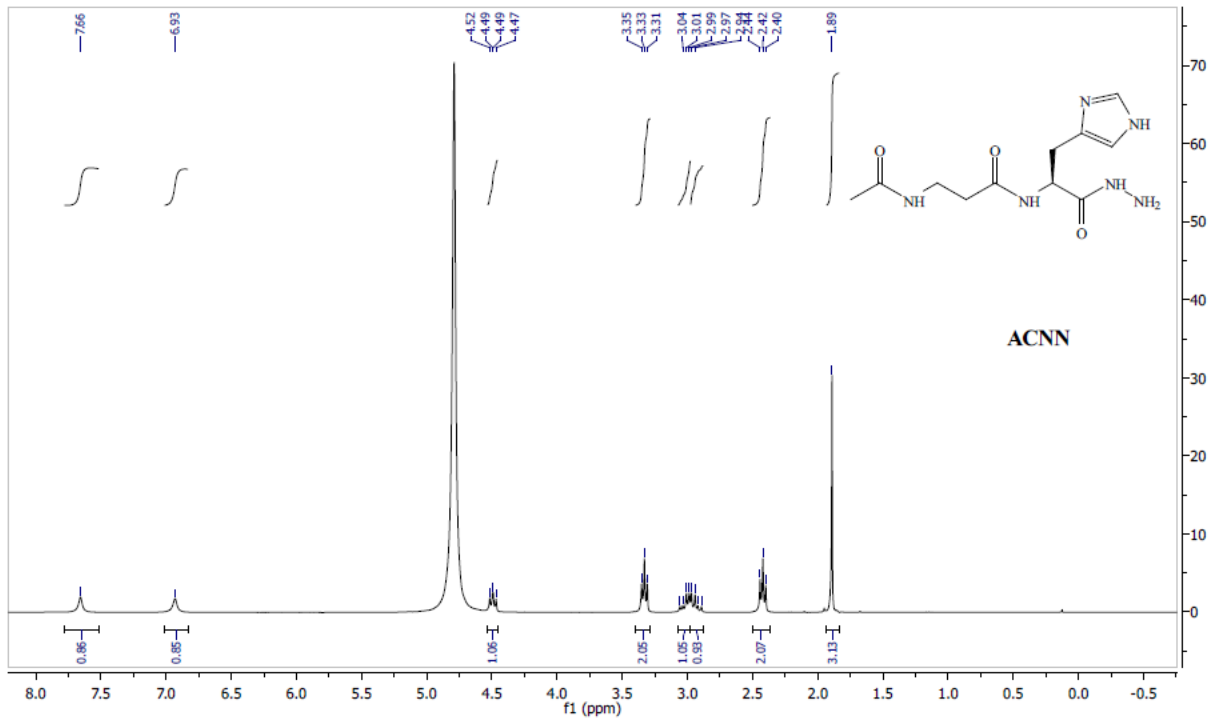
133.8, 119.6, 53.3, 39.1, 39.0, 30.3, 20.5. IR (ATR) 3350, 3276, 3181, 3024, 2936, 1632, 1560, 1425, 1338 cm^{-1} . MS (FAB) m/z 283.3 (M+H)⁺. HRMS (FAB) : Calcd for $\text{C}_{11}\text{H}_{19}\text{N}_6\text{O}_3$: 283.1519, Found 283.1528.

NMR Spectrum

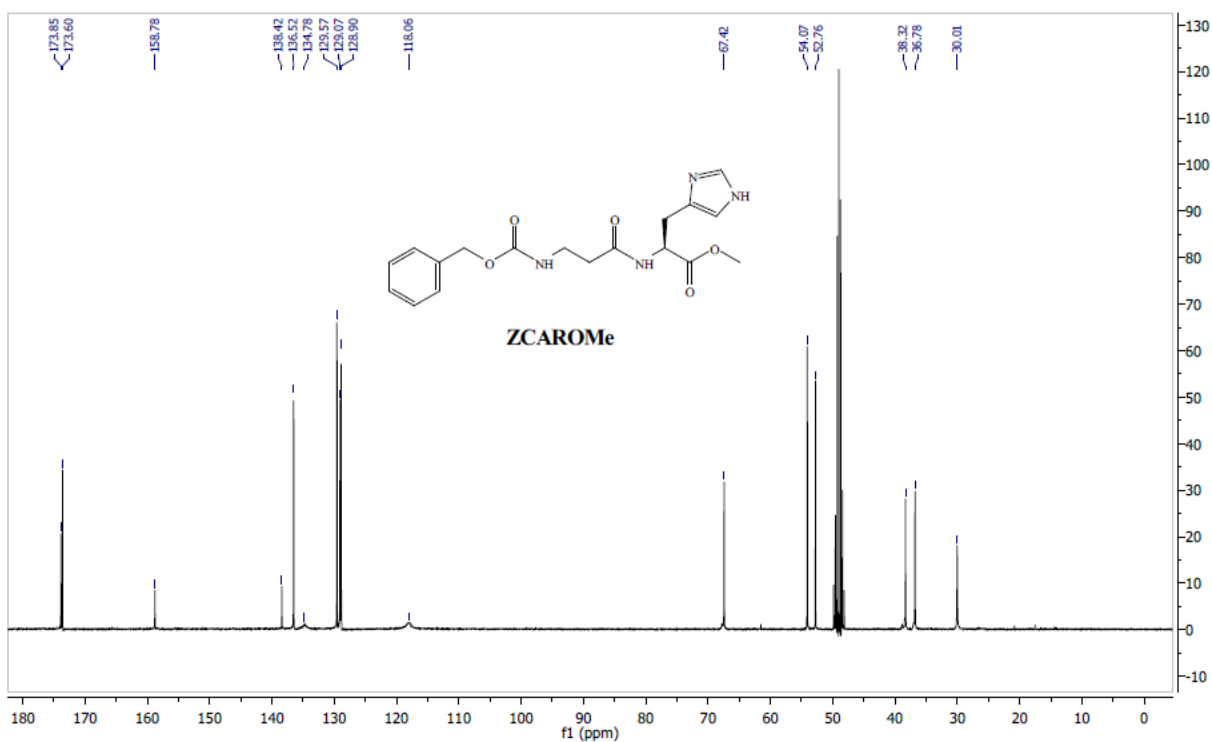
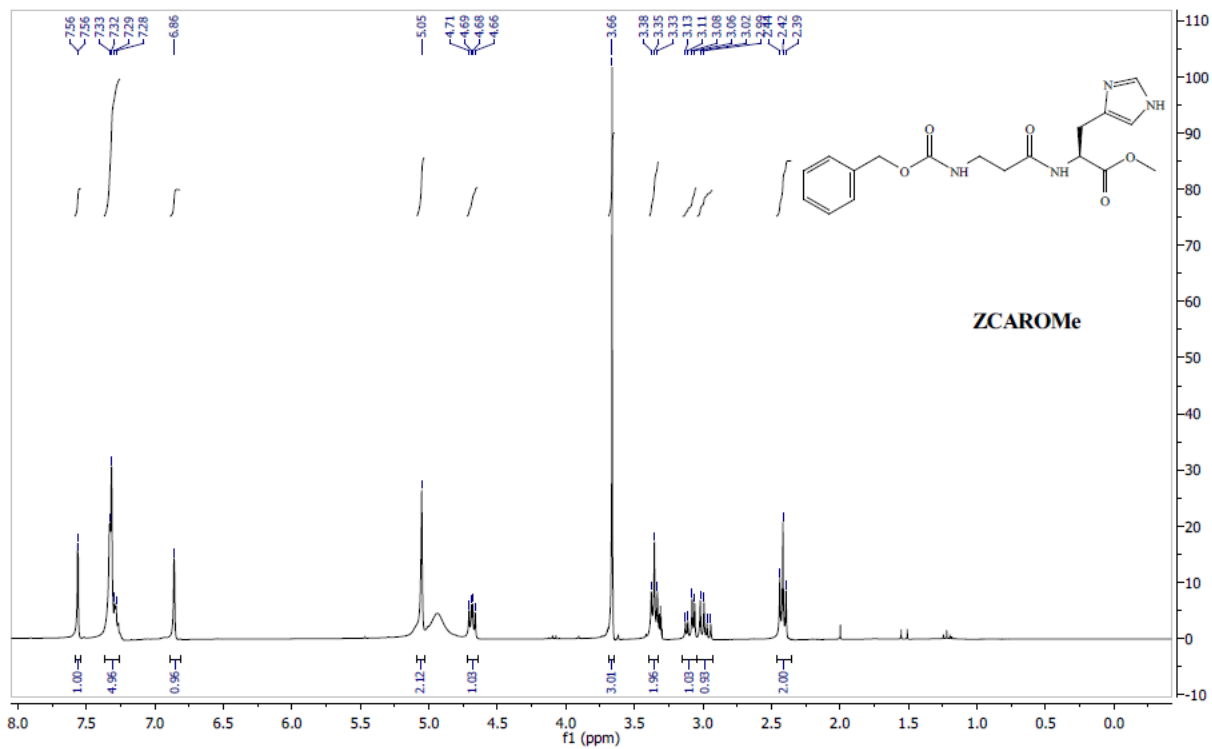
Ac-Carnosine-OMe



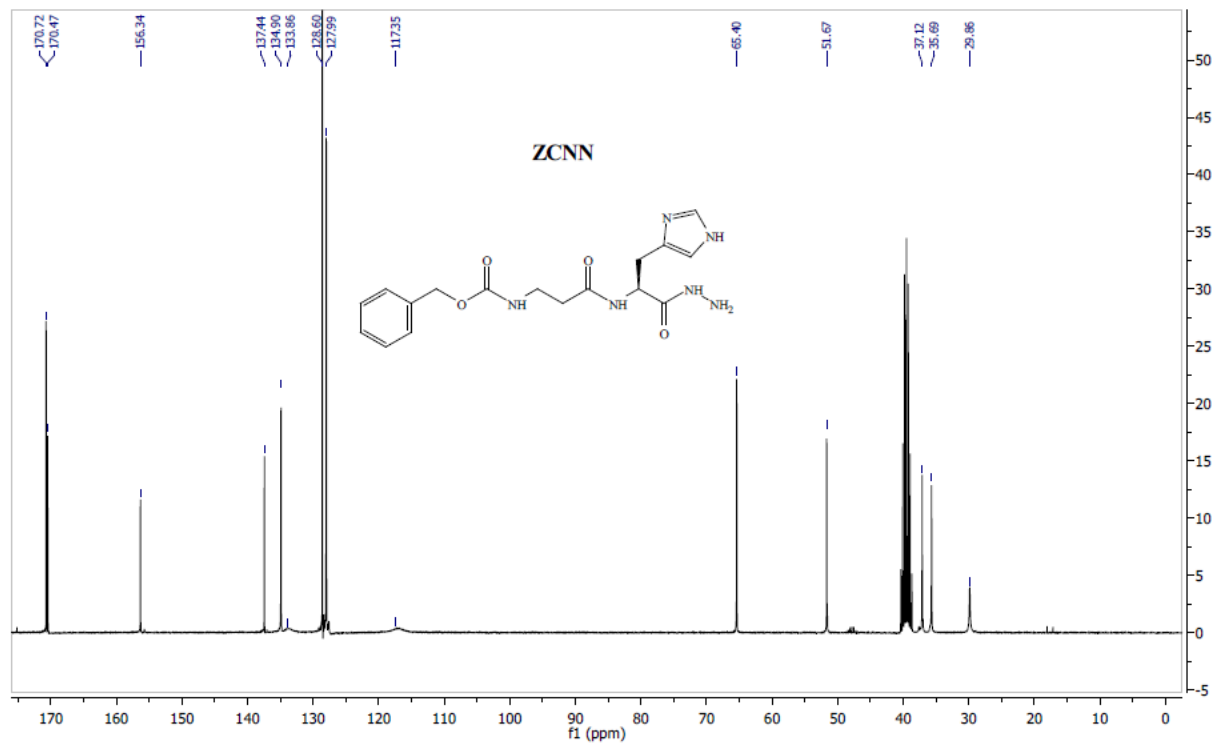
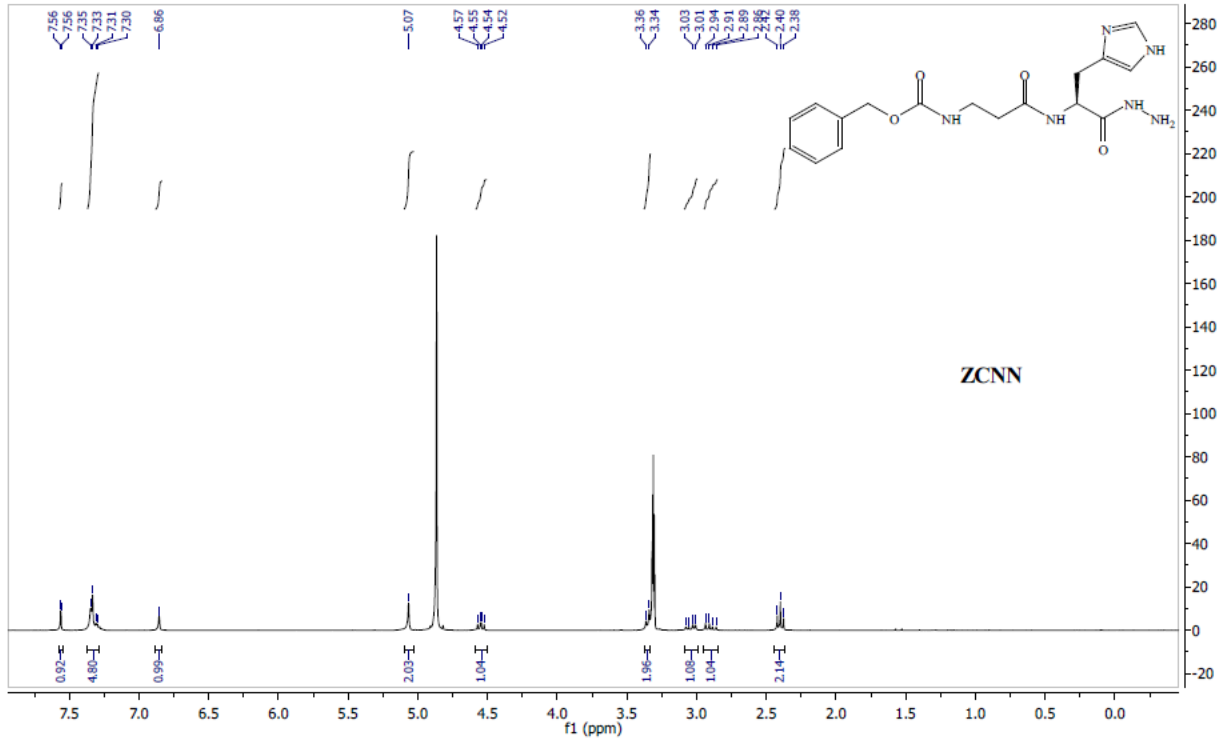
ACNN



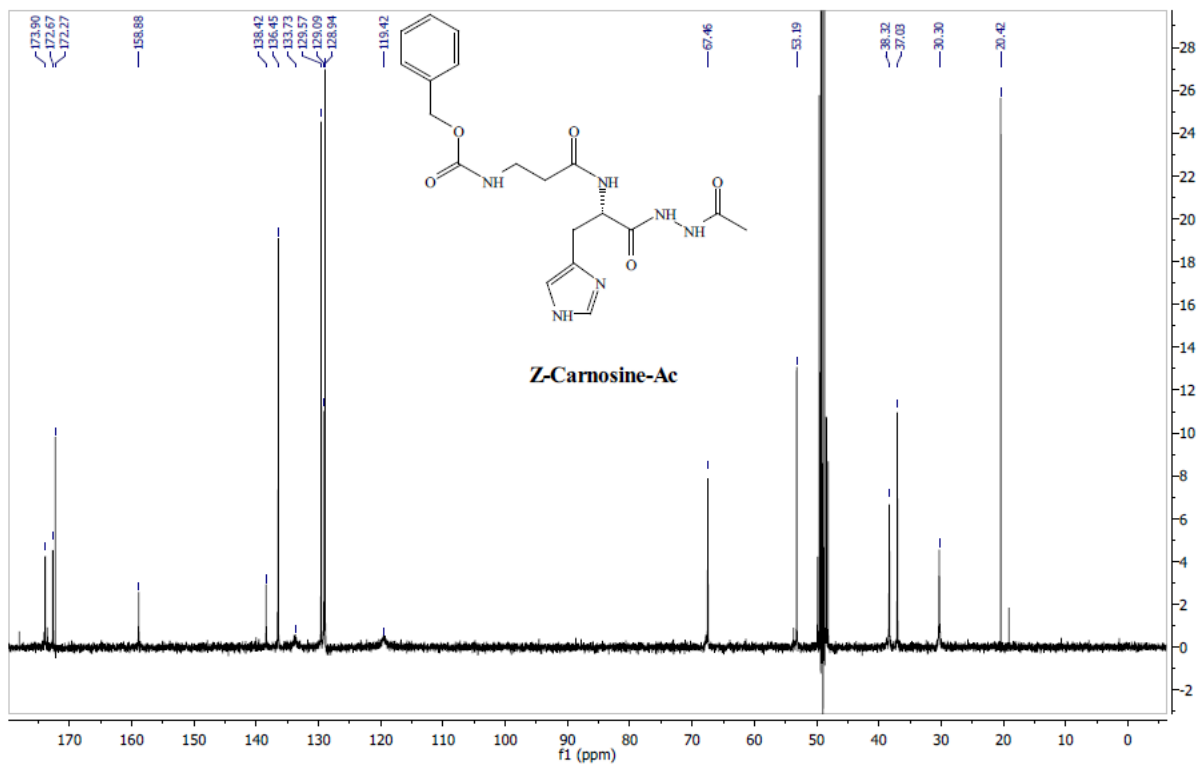
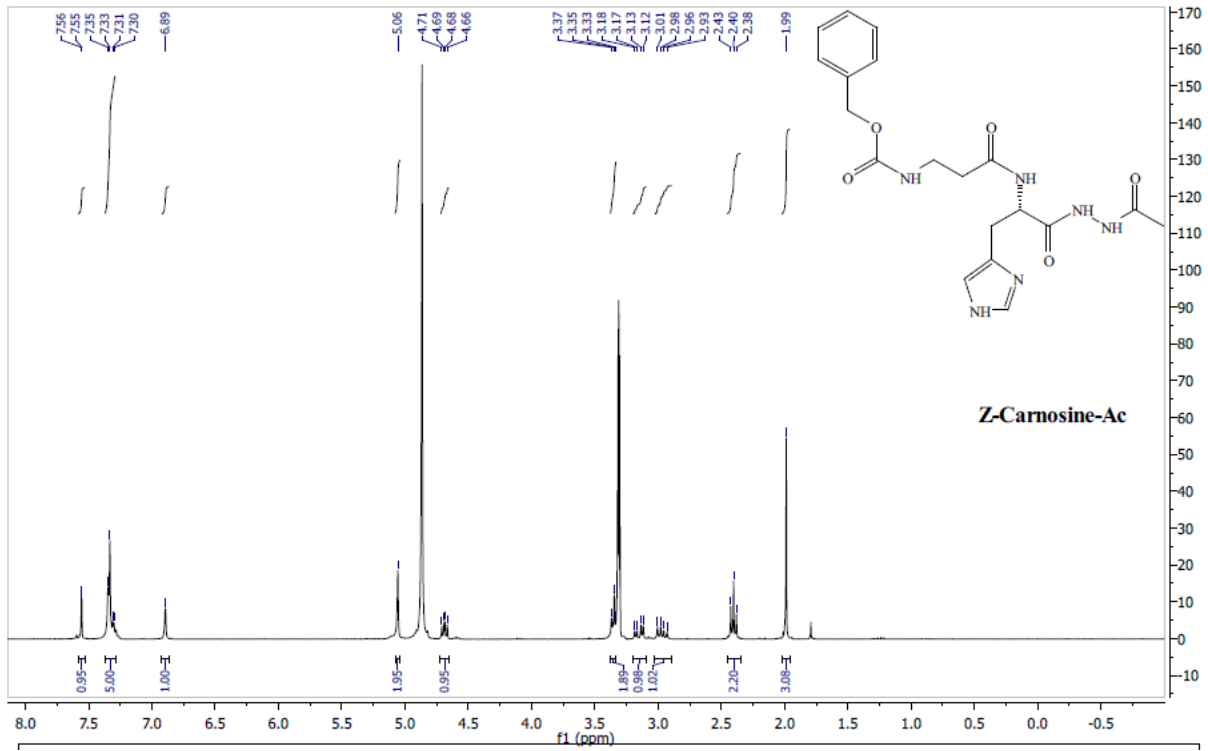
Cbz-Carnosine-OMe



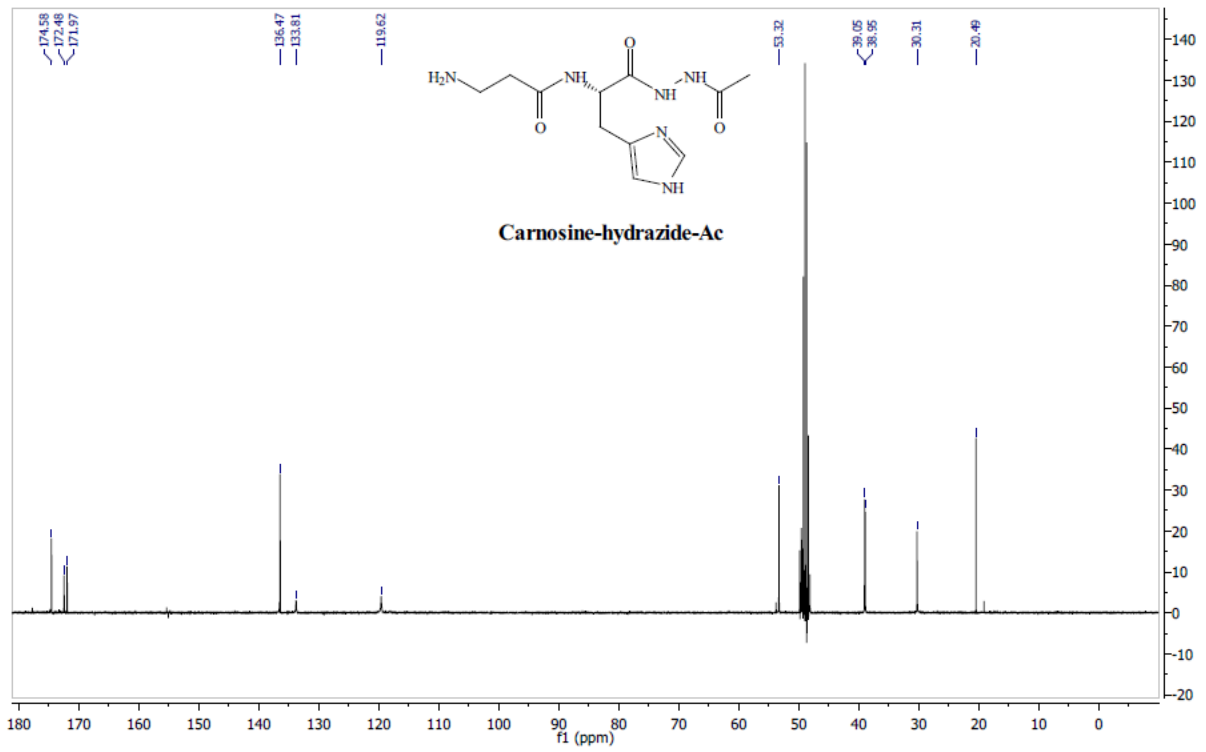
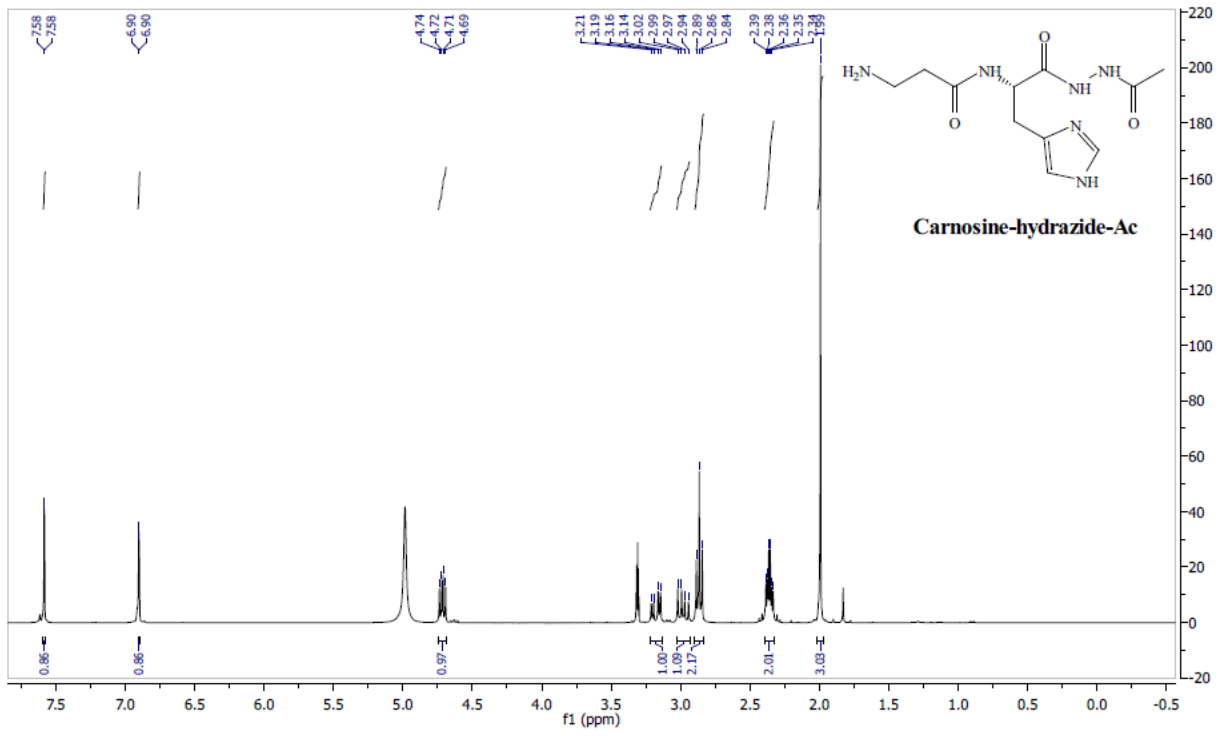
Cbz-Carnosine-NHNH₂



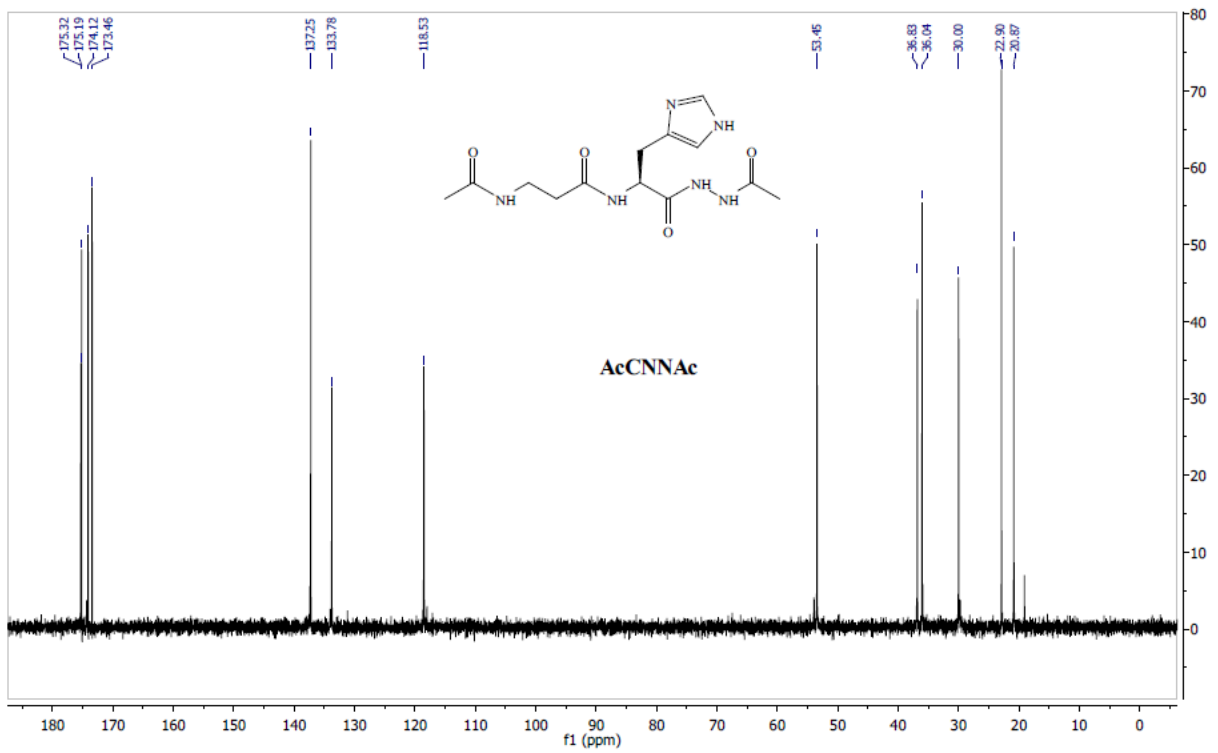
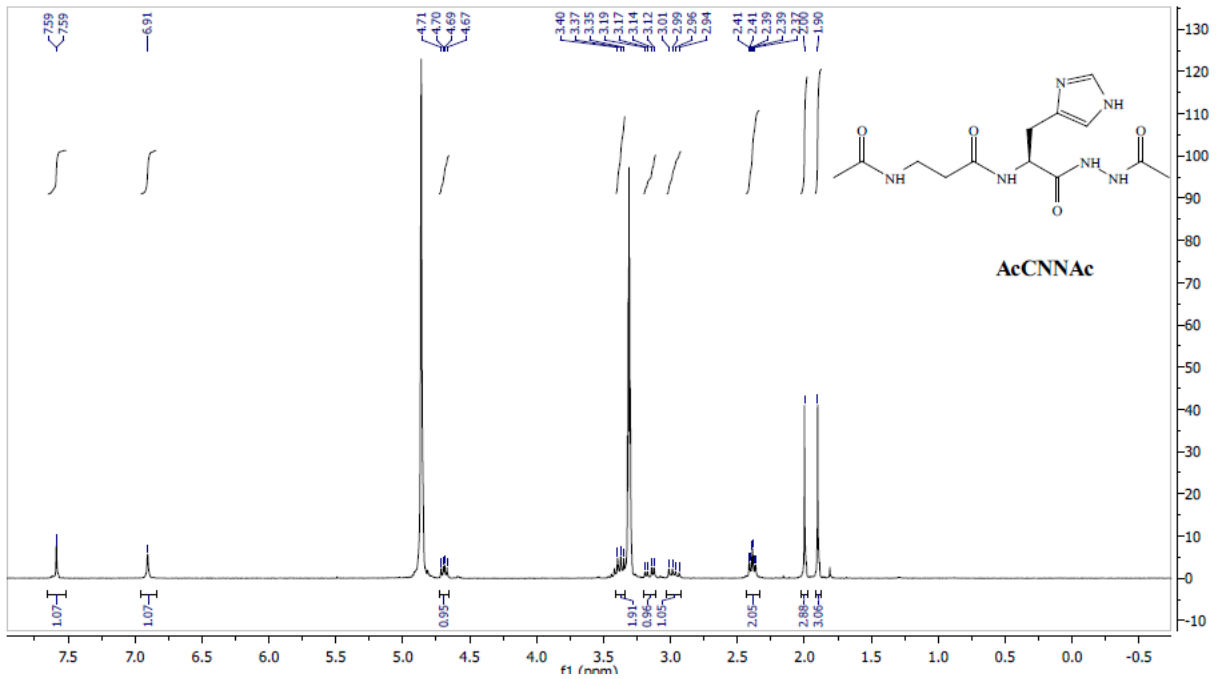
Cbz-Carnosine-Ac



CNNA



ACNNA



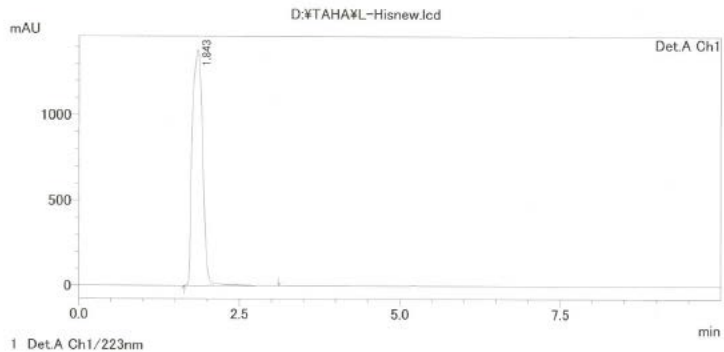
HPLC Purity Test

L-His

==== Shimadzu LCsolution 分析レポート ====

分析者 : System Administrator
サンプル名 : L-His
サンプルID : 1
トレイ番号 : 1
バイアル番号 : 1
注入量 : 50 uL
データファイル : L-Hisnew.lcd
メソッドファイル : TAHA.lcm
バッチファイル : HCARHH.lcb
レポートファイル : Default.lcr
分析日時 : 2014/10/31 14:45:42
解析日時 : 2014/10/31 14:55:46

<クロマトグラム>



ピークテーブル

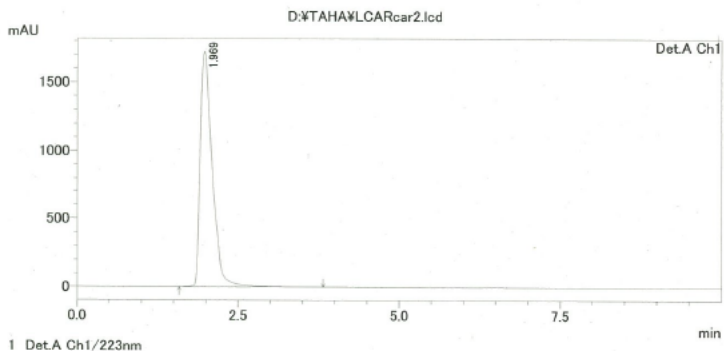
検出器A Ch1 223nm	ピーク#	保持時間	面積	高さ	面積%	高さ%
	1	1.843	15443585	1382151	100.000	100.000
	合計		15443585	1382151	100.000	100.000

L-CAR

==== Shimadzu LCsolution 分析レポート ====

分析者 : System Administrator
サンプル名 : L-CARcar
サンプルID : 001
トレイ番号 : 1
バイアル番号 : 1
注入量 : 50 uL
データファイル : L-CARcar2.lcd
メソッドファイル : TAHA.lcm
バッチファイル :
レポートファイル : Default.lcr
分析日時 : 2014/11/20 12:17:47
解析日時 : 2014/11/20 12:27:50

<クロマトグラム>



ピークテーブル

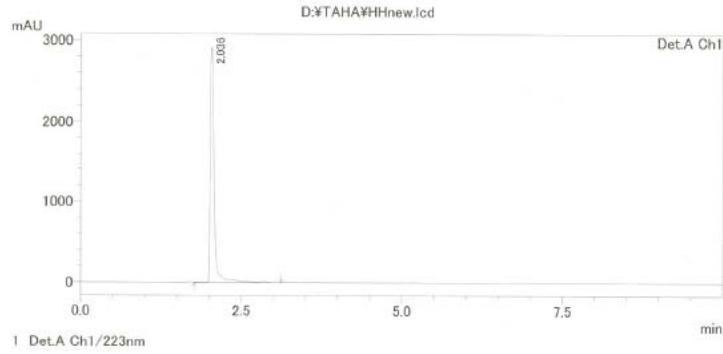
検出器A Ch1 223nm	ピーク#	保持時間	面積	高さ	面積%	高さ%
	1	1.969	22349714	1715419	100.000	100.000
	合計		22349714	1715419	100.000	100.000

HH

==== Shimadzu LCsolution 分析レポート ====

分析者 : System Administrator
サンプル名 : HH
サンプルID : 3
トレイ番号 : 1
バイアル番号 : 3
注入量 : 50 uL
データファイル : HHnew.lcd
メソッドファイル : TAHA.lcm
バッチファイル : HCARHH.lcb
レポートファイル : Default.lcr
分析日時 : 2014/10/31 15:06:32
解析日時 : 2014/10/31 16:34:09

<クロマトグラム>



ピークテーブル

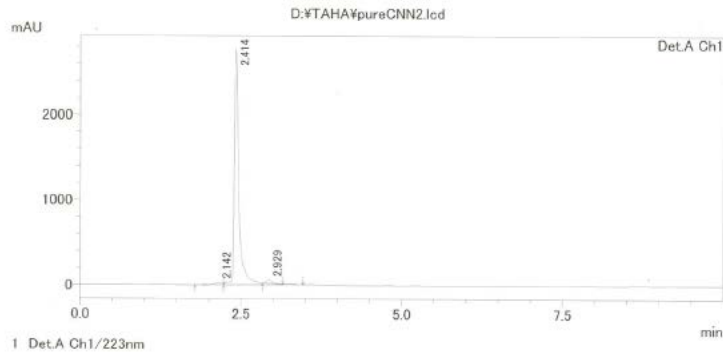
ピーク#	保持時間	面積	高さ	面積%	高さ%
1	2.036	12773796	2877401	100.000	100.000
合計		12773796	2877401	100.000	100.000

CNN

==== Shimadzu LCsolution 分析レポート ====

分析者 : System Administrator
サンプル名 : pureCNN
サンプルID : 001
トレイ番号 : 1
バイアル番号 : 1
注入量 : 50 uL
データファイル : pureCNN2.lcd
メソッドファイル : TAHA.lcm
バッチファイル :
レポートファイル : Default.lcr
分析日時 : 2014/11/16 21:09:56
解析日時 : 2014/11/16 21:19:58

<クロマトグラム>



ピークテーブル

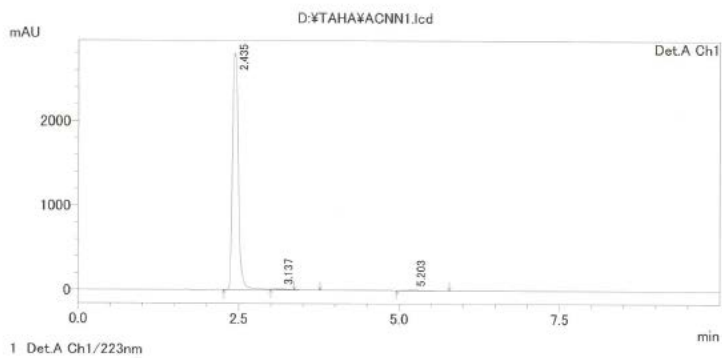
ピーク#	保持時間	面積	高さ	面積%	高さ%
1	2.142	265614	28564	1.819	1.024
2	2.414	14068987	2723764	96.327	97.599
3	2.929	270883	38447	1.855	1.378
合計		14605484	2790775	100.000	100.000

ACNN

==== Shimadzu LCsolution 分析レポート ====

分析者 : System Administrator
サンプル名 : ACNN
サンプルID : 5
トレイ番号 : 1
バイアル番号 : 5
注入量 : 50 uL
データファイル : ACNN1.lcd
メソッドファイル : TAHA.lcm
バッチファイル : HCARHH.lcb
レポートファイル : Default.lcr
分析日時 : 2014/10/31 11:46:18
解析日時 : 2014/10/31 11:56:21

<クロマトグラム>



検出器A Ch1 223nm

ピーク#	保持時間	面積	高さ	面積%	高さ%
1	2.435	18252353	2784546	99.145	99.436
2	3.137	94115	11208	0.511	0.400
3	5.203	63308	4576	0.344	0.163
合計		18409777	2800329	100.000	100.000

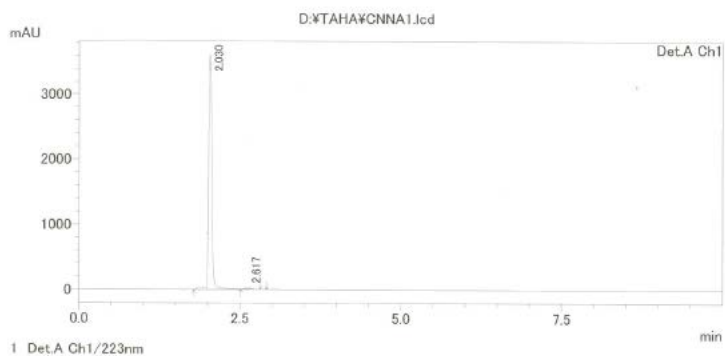
ピークテーブル

CNNA

==== Shimadzu LCsolution 分析レポート ====

分析者 : System Administrator
サンプル名 : CNNA
サンプルID : 6
トレイ番号 : 1
バイアル番号 : 6
注入量 : 50 uL
データファイル : CNNA1.lcd
メソッドファイル : TAHA.lcm
バッチファイル : HCARHH.lcb
レポートファイル : Default.lcr
分析日時 : 2014/10/31 11:56:43
解析日時 : 2014/10/31 16:39:03

<クロマトグラム>



検出器A Ch1 223nm

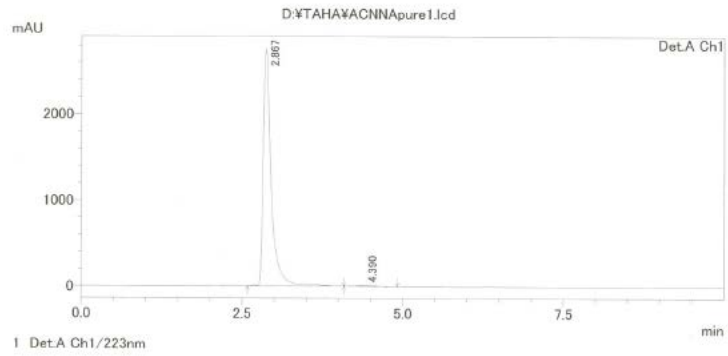
ピーク#	保持時間	面積	高さ	面積%	高さ%
1	2.030	13194149	3569497	98.674	99.032
2	2.617	177264	34907	1.326	0.968
合計		13371413	3604404	100.000	100.000

ピークテーブル

==== Shimadzu LCsolution 分析レポート ====

分析者 : System Administrator
 サンプル名 : ACNNApure
 サンプルID : 001
 トレイ番号 : 1
 バial番号 : 1
 注入量 : 50 uL
 データファイル : ACNNApure1.lcd
 メソッドファイル : TAHA.lcm
 バッチファイル :
 レポートファイル : Default.lcr
 分析日時 : 2014/11/16 19:53:08
 解析日時 : 2014/11/16 20:03:13

<クロマトグラム>



ピークテーブル

検出器A Ch1 223nm	ピーク#	保持時間	面積	高さ	面積%	高さ%
	1	2.867	24203166	2725845	99.645	99.857
	2	4.390	86249	3892	0.355	0.143
	合計		24289414	2729738	100.000	100.000